ChemistrySelect

Research Article
doi.org/10.1002/slct.202504720

Chemistry Europe
European Chemical Societies Publishing

www.chemistryselect.org

Targeting *Plasmodium Falciparum* Asexual and Sexual Stages with Melatonin-Based Indole Compounds

Abhinab Mohanty,[a] Lamark Carlos I,[b] Euzébio Guimarães Barbosa,[b] Alessandro Kappel Jordão,[b] and Celia R. S. Garcia*[a]

The effectiveness of current treatments against malaria, particularly artemisinin-based combination therapies (ACTs), is increasingly jeopardized by the emergence of drug resistance, underscoring the urgent need for novel antimalarial agents. Indole-based compounds, including melatonin derivatives, show promise in influencing parasite development, although their exact mechanisms of action remain elusive. In this study, we synthesized and evaluated a series of 1*H*-1,2,3-triazole and benzene ring derivatives derived from melatonin (**2**) and tryptamine (**9**). Using copper(I)-catalyzed azide-alkyne cycloaddition (CuAAC), we produced **20** compounds, **16** of which are novel, and tested their antimalarial efficacy against *Plasmodium Falciparum* (*P. falciparum*) 3D7 and a genetically modified strain lacking serpentine receptor 25 (PfSR25KO). Among these compounds, (**13**), (**7**), and (**8**) exhibited notable anti-plasmodial activity, with IC_{50} values of 33.38, 31.92, and 11.57 µM, respectively, with favorable selectivity indexes (SI). Investigation into their effects on the parasite's sexual stages revealed that compound (**13**) demonstrated significant gametocidal activity. When tested with melatonin, these compounds exhibited diverse interactions: some mimicked melatonin's effects, while others acted as competitive inhibitors. This suggests their mode of action involves modulating melatonin-related signaling pathways in the parasite. These findings highlight the potential of triazole-based indole derivatives as promising candidates for therapeutic interventions and blocking malaria transmission.

1. Introduction

Malaria continues to be a significant global health issue, affecting millions each year. The parasite *Plasmodium falciparum* (*P. falciparum*) is the leading cause of malaria-related deaths, with artemisinin-based combination therapy (ACT) currently recommended as the first-line treatment for uncomplicated cases. ACT combines artemisinin or its derivatives with partner drugs with different mechanisms and longer half-lives to combat resistance. However, the emergence of ACT-resistant parasites poses a severe threat, with concerns that malaria mortality rates could rise to levels seen in the 1980s during the spread of chloroquine resistance in Africa[1] As resistance to chloroquine and artemisinin spreads, discovering new compounds to replace traditional treatments has become urgent. Promising candidates include compounds with unique chemical structures and mechanisms, such as 4-aminoquinolines, antifolates, aryl-amino alcohols, naphthoquinones, antibiotics, and endoperoxides.[2,3]

Melatonin (*N*-acetyl-5-methoxytryptamine, 2), a hormone derived from L-tryptophan (1), primarily synthesized by the pineal gland, plays a regulatory role in various physiological processes and is present across multiple organisms, from plants and fungi to mammals.[4,5] In *P. falciparum* and *P. chabaudi*, melatonin has been found to synchronize the intraerythrocytic developmental cycle of these parasites, which is believed to occur through a signaling pathway involving phospholipase C and inositol triphosphate, resulting in increased cytosolic calcium and cyclic AMP levels.[6–8] Synthetic analogs of melatonin and related indole compounds, such as *N*-acetyl-serotonin, can modulate parasitemia in vitro.[8–10] Certain compounds, like 8-oxo-tryptamine, exhibit antimalarial properties, while melatonin receptor antagonists like luzindole disrupt intracellular calcium oscillations and cyclic AMP production, impairing parasite development during the asexual stages.[11,12] Additional research has shown that C2-arylalkanimino tryptamine derivatives and biofunctionalized indole compounds, such as Flinderoles and Borreverines, may inhibit melatonin-driven parasite synchronization and hinder intraerythrocytic development.[13–15] Another promising compound, spiroindolone KAE609, which exhibits potent antimalarial activity, is undergoing phase II clinical trials.[16]

Exploring new therapeutic agents against malaria remains essential due to the challenges of drug resistance and the need for more effective treatments.[17] In this context, our research aimed to synthesize new indole-derived compounds

[a] *A. Mohanty, C. R. S. Garcia*
Department of Clinical and Toxicological Analyses, School of Pharmaceutical Sciences, University of São Paulo, São Paulo, SP 05508-000, Brazil
E-mail: cgarcia@usp.br

[b] *L. Carlos I, E. G. Barbosa, A. K. Jordão*
Department of Pharmacy, Federal University of Rio Grande do Norte, Natal, RN 59012-570, Brazil

Supporting information for this article is available on the WWW under https://doi.org/10.1002/slct.202504720

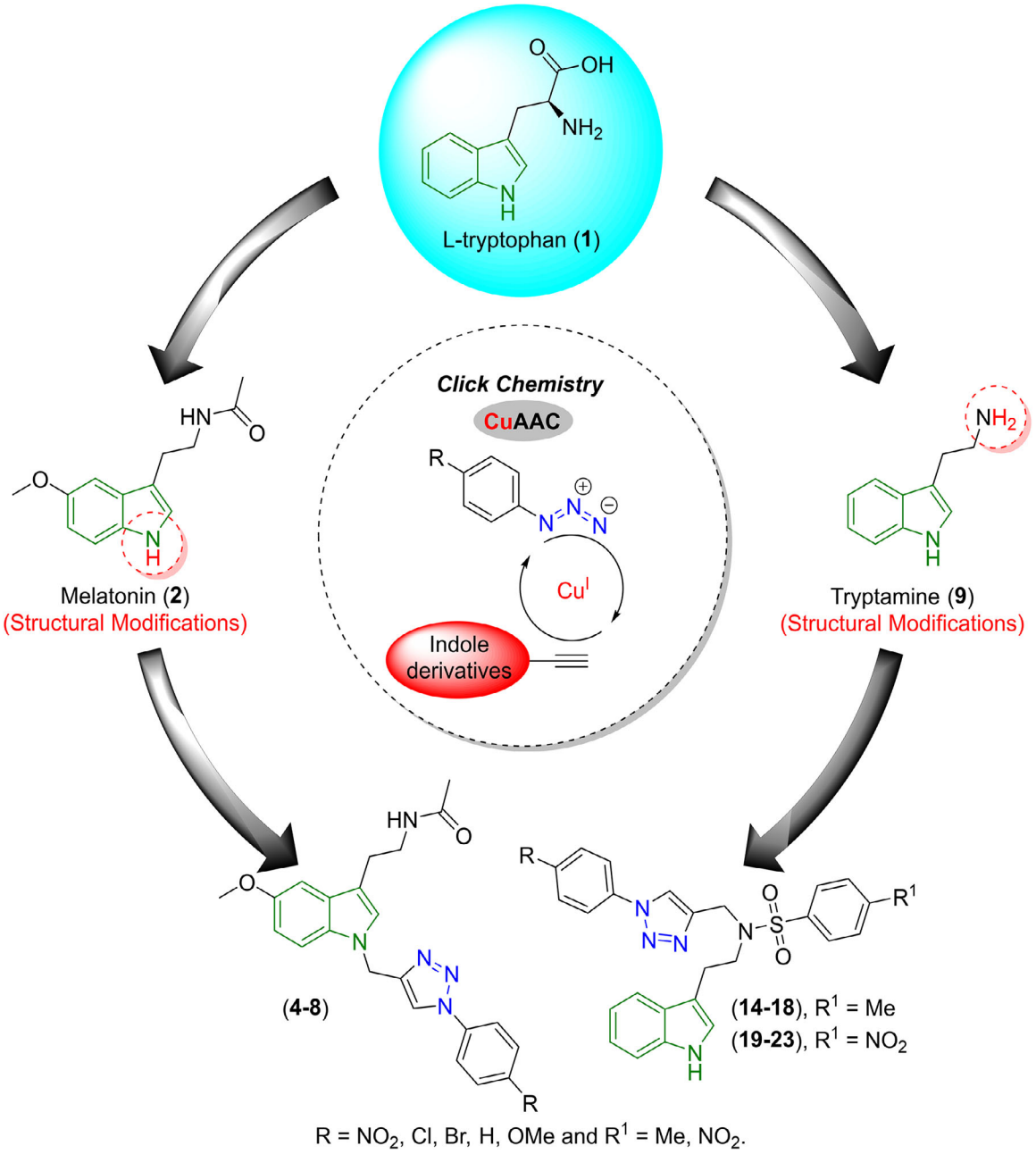

Figure 1. Structural analogues derived from melatonin (**4**–**8**) and tryptamine (**14**–**23**).

featuring 1*H*-1,2,3-triazole and benzene rings with various substituents, especially by making targeted structural modifications to melatonin (**2**) and tryptamine (**9**) molecules. The synthesis was conducted using the CuAAC methodology, catalyzed by copper (I) ("click chemistry"), as first described by Sharpless et al.[18,19] This versatile and efficient approach enables molecular fragments to connect, enhancing their pharmacological properties for medicinal applications. Furthermore, recent scientific literature reports the antimalarial activity of 1H-1,2,3-triazoles derived from indole derivatives.[20–22] Our study assessed the antimalarial potential of these newly synthesized compounds, focusing on the effects of aromatic substitution patterns and the influence of the triazole ring on derivatives of melatonin (**4**–**8**) and tryptamine (**14**–**23**) (Figure 1).

This study examined the antimalarial activity of 20 melatonin-based compounds against the *P. falciparum* 3D7 strain and a modified strain with a serpentine receptor 25 knockout (SR25KO). We also assessed the impact of these compounds and melatonin on *P. falciparum* parasitemia at sub-optimal doses. Moreover, we have selected the best compounds from this series to investigate their ability to block *P. falciparum* sexual development. These findings underscore the potential of melatonin-based indole compounds, especially those designed to interfere with melatonin signaling pathways, as promising candidates in the search for novel antimalarial therapies.[23–25]

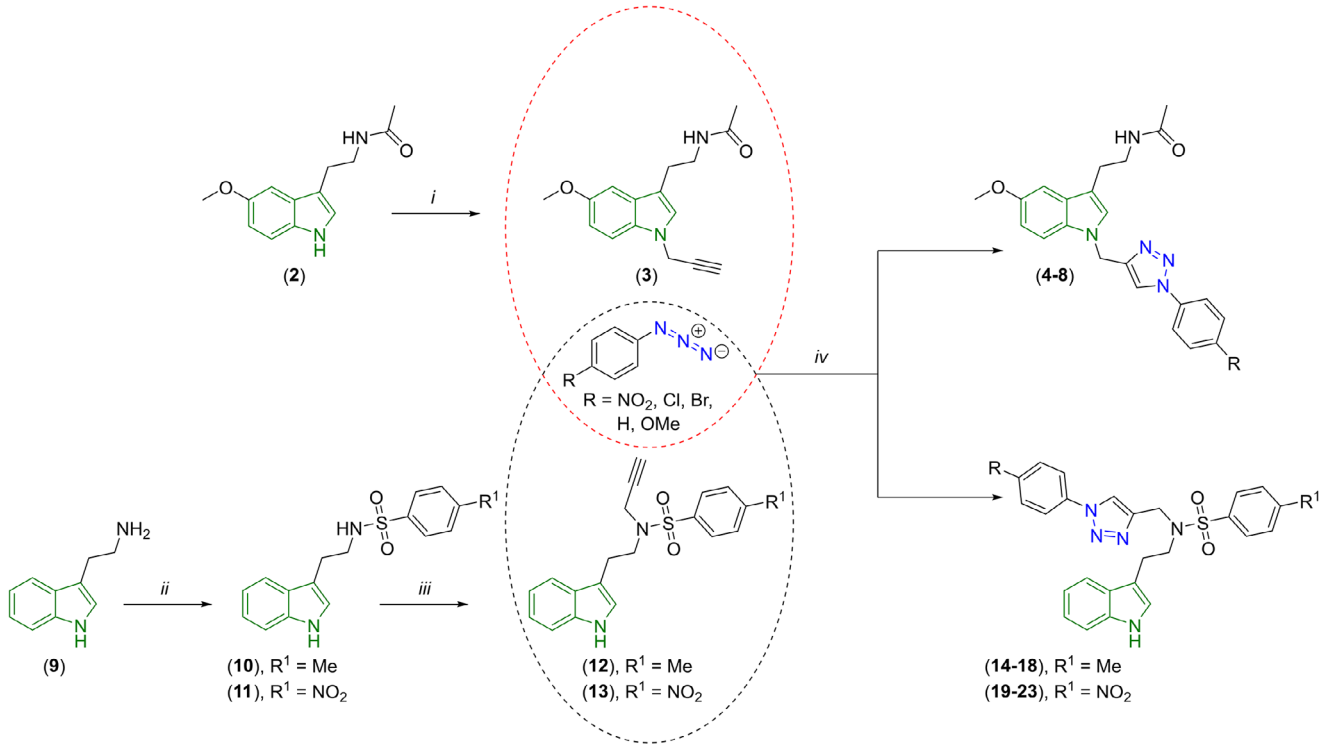

Reactions conditions: *i)* NaOH (1.2 equiv.) in DMF (5 mL), 0 °C, 2h; 80% (w/w) propargyl bromide in toluene (2.0 equiv.), rt, 2h. *ii)* Benzenesulfonyl chloride *p*-substituted (R^1 = Me or NO_2)(1.0 equiv.), Et_3N (1.2 equiv.) in THF (15 mL), 0 to 45 °C, 4h. *iii)* K_2CO_3 (1.2 equiv.) in DMF (10 mL), 80% (w/w) Propargyl bromide in toluene (1.2 equiv.), rt, 16h. *iv)* Aryl azides substituted (1.05 equiv.), $CuSO_4.5H_2O$ (1.0 equiv.), sodium ascorbate (0.5 equiv.) in THF/H_2O 1:1 (v/v, 10 mL), rt.

Figure 2. Synthesis of two families of 1*H*-1,2,3-triazoles derived from indole (**4**--**8**) and (**14**--**23**).

2. Results

2.1. Synthesis and Characterization of Derivatives from Melatonin and Tryptamine

We successfully synthesized triazole derivatives from melatonin and tryptamine using a stepwise approach that showcased the versatility of copper(I)-catalyzed azide-alkyne cycloaddition (CuAAC). Alkylation generated a terminal alkyne intermediate for melatonin, which was then reacted with various aromatic azides to produce triazole derivatives (**4**–**8**) in good yields (68%–91%). Similarly, tryptamine was first converted into sulfonamide intermediates using p-substituted benzenesulfonyl chlorides, followed by alkylation with propargyl bromide to create acetylene intermediates. These intermediates were then subjected to CuAAC, yielding triazole derivatives (**14**–**23**) with yields ranging from 59%–91% (Figure 2). The CuAAC method proved robust and adaptable, accommodating a range of aromatic substituents with different electronic properties, making it an effective tool for expanding chemical diversity.

The structures of all synthesized compounds were confirmed through ^{1}H NMR, ^{13}C NMR, and FT-IR spectroscopy. We observed clear triazole proton signals in the ^{1}H NMR spectra, distinct carbon peaks in the ^{13}C NMR, and characteristic sulfonamide and triazole bands in the FT-IR. Melatonin derivatives consistently provided higher yields than tryptamine derivatives, likely due to steric and electronic factors affecting the latter's intermediates. Overall, the synthetic methods used in this study were efficient, reliable, and scalable, resulting in a diverse library of indole-based compounds. This work provides a strong foundation for further exploration of their biological activities, particularly in the search for new antimalarial treatments.

2.2. Anti-plasmodial Activity of Derivatives Against the Asexual Stages of *P. falciparum*

In our investigation into the antimalarial potential of this series of compounds, we began by evaluating their solubility in RPMI media, a standard aqueous culture medium used for growing *P. falciparum*. Ensuring solubility was a crucial first step to confirm the compounds were suitable for biological testing. Out of 20 compounds initially tested, **16** were found to dissolve in the medium at varying concentrations, while three of the remaining four compounds were deemed insoluble and excluded from further experiments. The final compound had previously published IC_{50} data and was not re-evaluated in this study.[24]

Next, we assessed the ability of the **16** soluble compounds to inhibit the growth of the asexual blood stages of *P. falciparum* using the well-characterized 3D7 strain of the parasite. Dose-response curves were generated for each compound, and their half-maximal inhibitory concentrations (IC_{50} values) were calculated to evaluate their efficacy. A comprehensive summary of the compound structures and corresponding IC_{50} values is provided in Table 1.

The majority of the compounds (**13** out of **16**) showed limited or no antimalarial activity. These compounds either had IC_{50}

Table 1. Determination of the anti-plasmodial activity of synthetic indole compounds in wild-type parasites (3D7) and the genetically modified strain PfSR25KO.

Compound	Structure	IC_{50} (μM) 3D7 strain[a)]	IC_{50} (μM) PfSR25KO strain[a)]
(3)	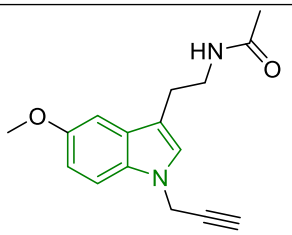	210 ± 26	
(4)	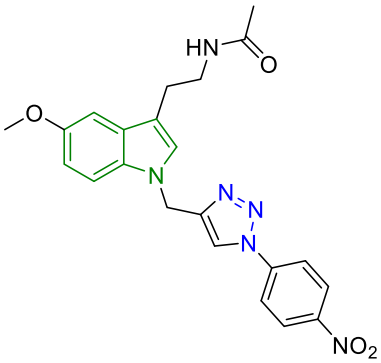	N.S[b)]	N.S[b)]
(5)	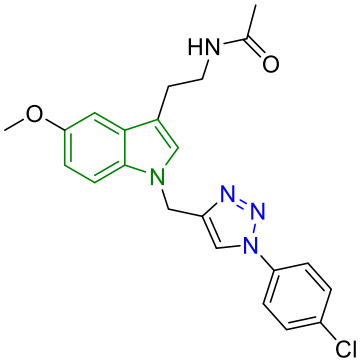	67 ± 5.1	
(6)	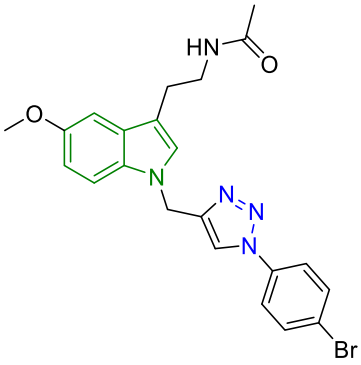	37 ± 14	
(7)	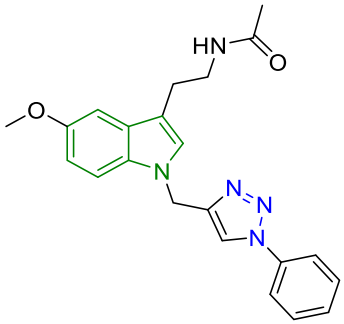	32 ± 6.4	26 ± 4.9

Table 1. (Continued)

Compound	Structure	IC_{50} (μM) 3D7 strain[a)]	IC_{50} (μM) PfSR25KO strain[a)]
(8)	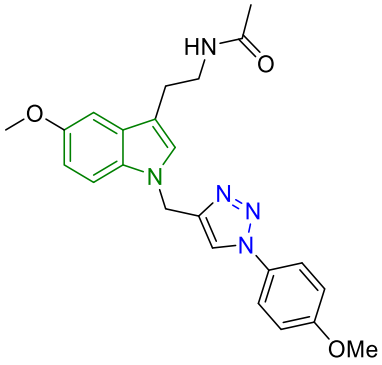	12 ± 1.9	15 ± 0.60
(10)	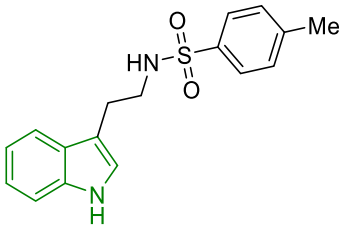	Data Published[24]	
(11)	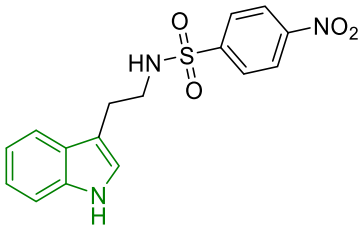	N.D[c)]	
(12)	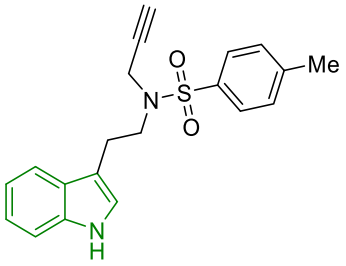	59 ± 2.9	
(13)	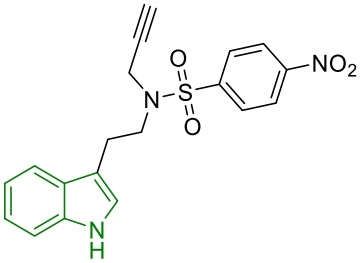	33 ± 1.5	38 ± 8.6
(14)	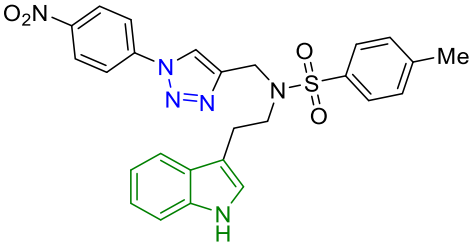	79 ± 18	

Table 1. (Continued)

Compound	Structure	IC_{50} (μM) 3D7 strain[a]	IC_{50} (μM) PfSR25KO strain[a]
(15)	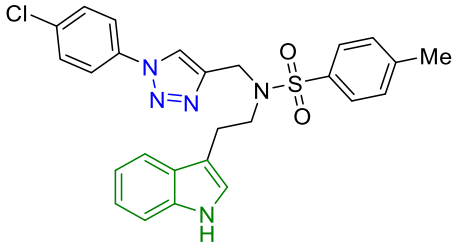	61 ± 8.3	
(16)	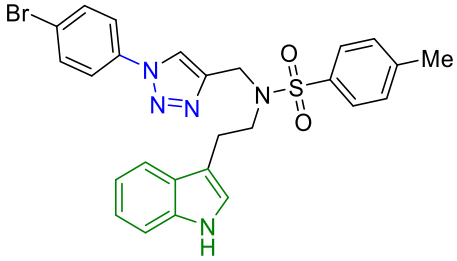	130 ± 5.1	
(17)	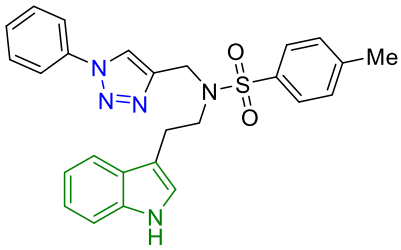	N.D[c]	
(18)	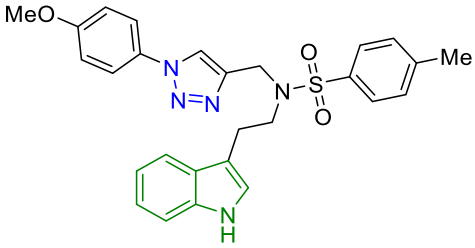	N.S[b]	N.S[b]
(19)	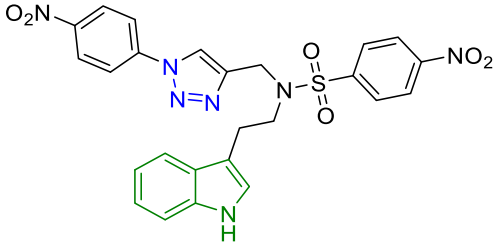	13 ± 4.4	
(20)	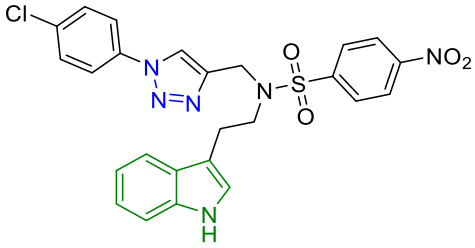	11 ± 4.2	

Table 1. (Continued)

Compound	Structure	IC_{50} (μM) 3D7 strain[a)]	IC_{50} (μM) PfSR25KO strain[a)]
(21)	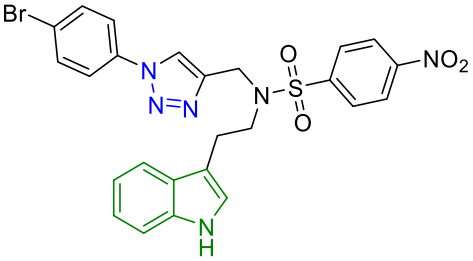	240 ± 29	
(22)	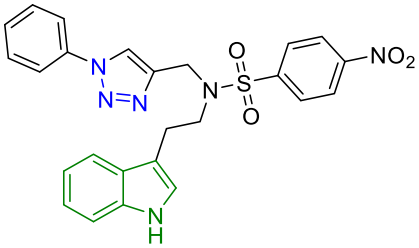	N.S[b)]	N.S[b)]
(23)	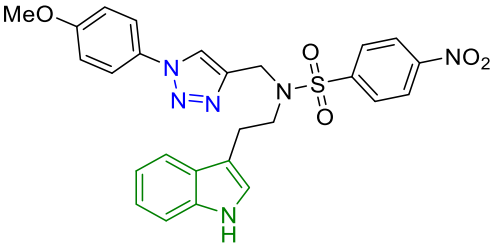	35 ± 0.95	
Chloroquine	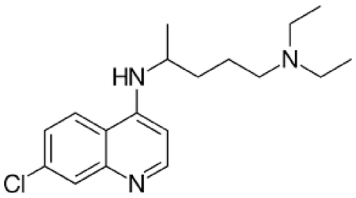	0.012 ± 0.0027	0.012 ± 0.0051

[a)] Values are the mean ± SD of biological repeat experiments performed in triplicate, reported to two significant figures.
[b)] Not soluble.
[c)] Not determined.

values exceeding the highest concentration tested or failed to demonstrate significant parasite inhibition at any tested dose (Figure S1). The compounds tested showed antimalarial activity with the IC_{50} values in the micromolar range. In contrast, three compounds, identified as (**13**), (**7**), and (**8**), displayed measurable antimalarial activity, with IC_{50} values of 33 ± 1.5 μM, 32 ± 6.4 μM, and 12 ± 1.9 μM, respectively (Figure 3). Among these, compound (**8**) emerged as the most potent, followed by (**7**) and (**13**). These results highlight the potential of these three compounds as promising candidates for further investigation, providing a strong foundation for future studies aimed at their optimization and development as antimalarial agents.

2.3. Differential Activity was not Observed Against the *P. falciparum* Knockout Strain for Serpentine Receptor 25 (PfSR25KO)

To investigate the mechanism of action of the three active indole-based compounds, we assessed their efficacy against a genetically modified *P. falciparum* strain, specifically the knockout strain for serpentine receptor 25 (PfSR25KO). This approach was aimed at determining whether the compounds exert their antimalarial effects through interaction with the SR25 receptor or its associated downstream signaling pathways. The IC_{50} values obtained against the PfSR25KO strain for compounds (**13**), (**7**), and (**8**) were 38 ± 8.6 μM, 26 ± 4.9 μM, and 15 ± 0.60 μM, respectively.

As shown in Figure 4, the compounds exhibited similar killing activity against both the wild-type 3D7 strain and the PfSR25KO strain, with no statistically significant differences observed based on *t*-test analysis. However, despite the lack of statistical significance, a trend was observed: compounds (**13**) and (**8**) showed a slight increase in IC_{50} in the PfSR25KO strain, while the knockout strain appeared to be more sensitive to compound (**7**). These findings suggest that the mechanism of action of these indole-based compounds does not involve the SR25 receptor or its downstream signaling pathways. Instead, it is likely that these compounds act through alternative molecular mechanisms, war-

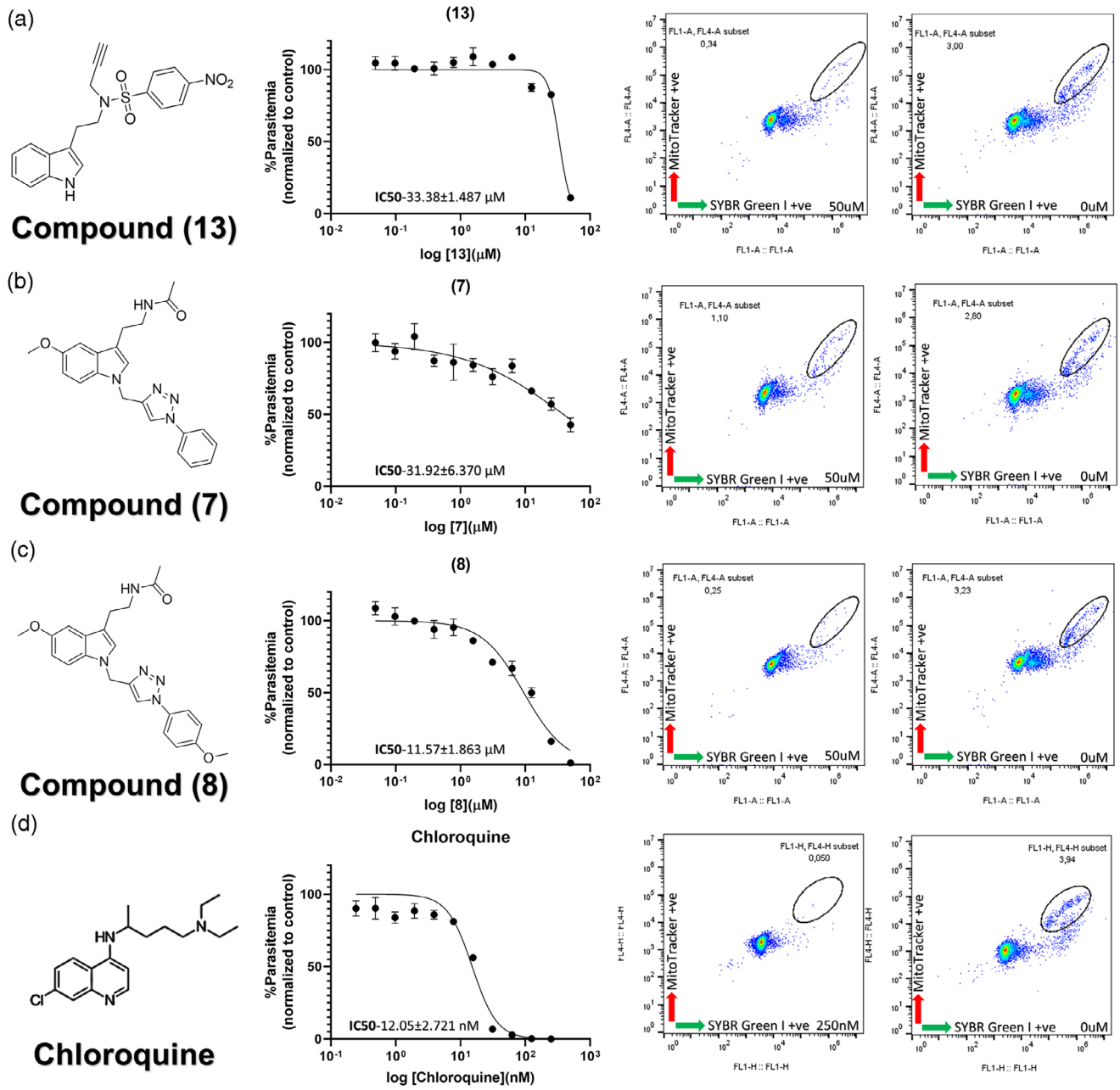

Figure 3. Determination of the anti-plasmodial activity of synthetic indole compounds in wild-type parasites (3D7). The figure represents the growth survival curves of *P. falciparum* in response to the three best compounds along with their IC_{50}s and cytometric dot-plot figures at their highest working concentration (left) to the lowest concentration (right). Panels a)–c) display three compounds: (**13**), (**7**), and (**8**). Panel d) illustrates the action of Chloroquine, which serves as the positive control in this experiment. The asynchronous culture of 3D7 was exposed to compounds for 72h. The parasitemia calculation was done by double-staining the parasites with SYBR Green I and MitoTracker to separate viable parasites from the population. Experiments were performed three independent times in triplicates. Error bars represent the standard deviation (SD).

ranting further investigation to fully elucidate their mode of action.

2.4. Compounds Effective Against *P. falciparum* are not Toxic Mammalian Cell Line HEK293T

We further evaluated the cytotoxicity of three compounds with promising antimalarial activity, specifically for (**13**), (**7**), and (**8**), to determine their effects on mammalian cells. Using the HEK293T cell line, survival assays indicated that all three compounds were non-toxic at the tested concentrations, as evidenced by their survival curves (Figure 5). The Selectivity Index (SI), calculated as the ratio of cytotoxic concentration (CC_{50}) in HEK293T cells to the effective antimalarial concentration (IC_{50}), further supports these observations. Since no cytotoxicity was observed at the highest concentration tested (50 µM), and higher concentrations could not be assessed due to solubility limitations, precise SI values could not be determined. Instead, we report lower-bound estimates: >1.49 for (**13**), >1.56 for (**7**), and >4.32 for (**8**), indicating selectivity toward the parasite only.

Research Article
doi.org/10.1002/slct.202504720

Chemistry Europe
European Chemical Societies Publishing

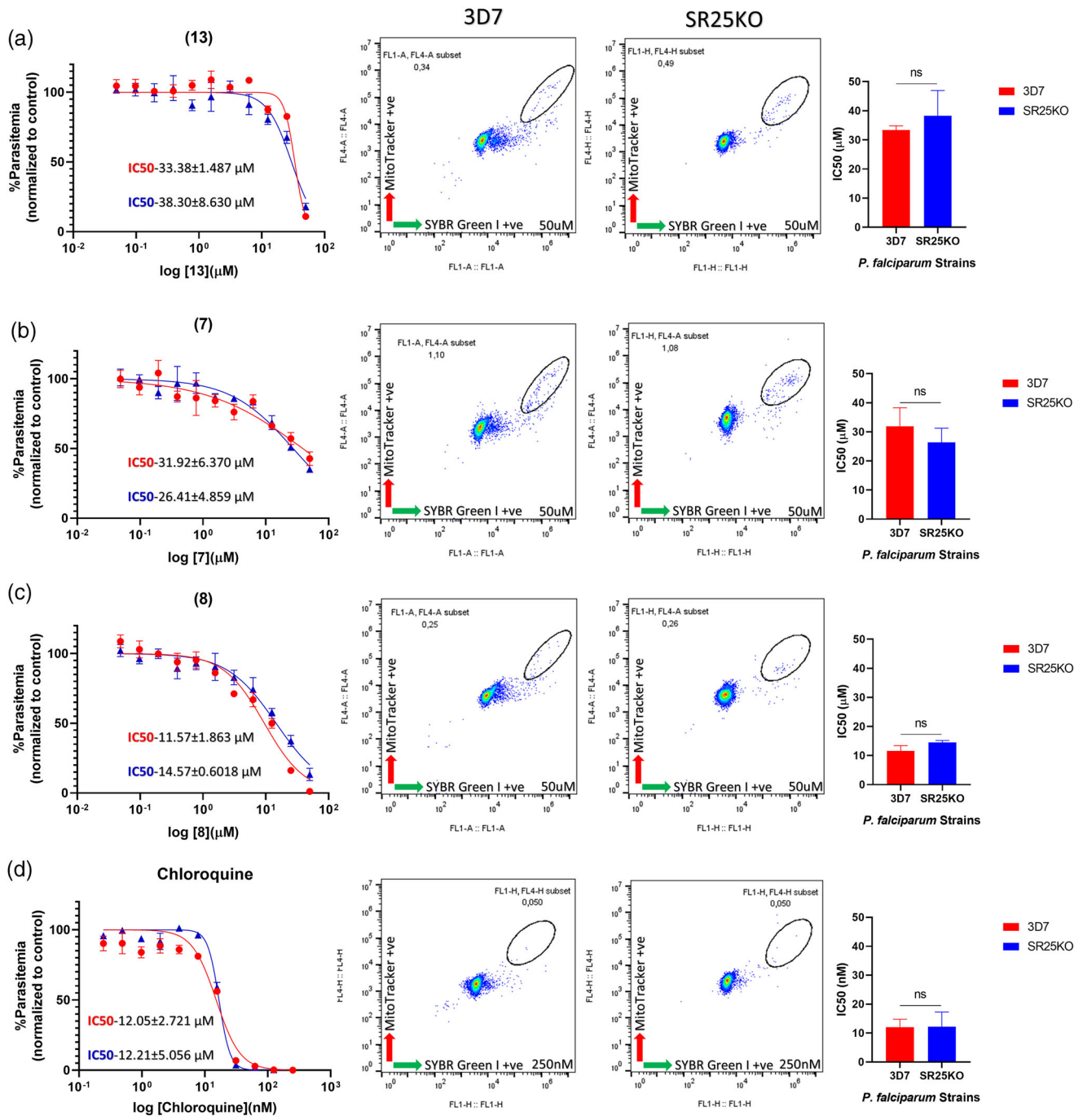

Figure 4. Indole compounds do not affect the SR25 receptor and its associated signaling pathway as a mechanism of anti-plasmodial action. This figure demonstrates that the three indole-based compounds do not target the SR25 receptor or its associated signaling pathways as a mechanism of anti-plasmodial action. Panels a)–c) show the survival curves for compounds (**13**), (**7**), and (**8**), respectively, in response to treatment of both the wild-type 3D7 strain and the genetically modified PfSR25KO strain. Panel d) shows the activity of Chloroquine, which acts as the positive control in this experiment. The cytometric dot plots in the middle of the figure represent the results obtained at the highest working concentration of each compound for both strains. The bar graphs to the right summarize the differential IC_{50} values between the two strains, with statistical analysis performed using a *t*-test. Asynchronous cultures of both the 3D7 and PfSR25KO strains were exposed to each compound for 72 h. Parasitemia was assessed by double-staining the parasites with SYBR Green I and MitoTracker, allowing for the separation of viable parasites from the overall population. The dose-dependent activity of (**13**), (**7**), and (**8**) shows no significant difference between the two parasite strains. Findings suggest that the anti-plasmodial effects do not involve the SR25 receptor, indicating that alternative molecular targets may be responsible for their activity. Experiments were performed in triplicate across three independent trials. Error bars represent the standard deviation (SD) of the mean.

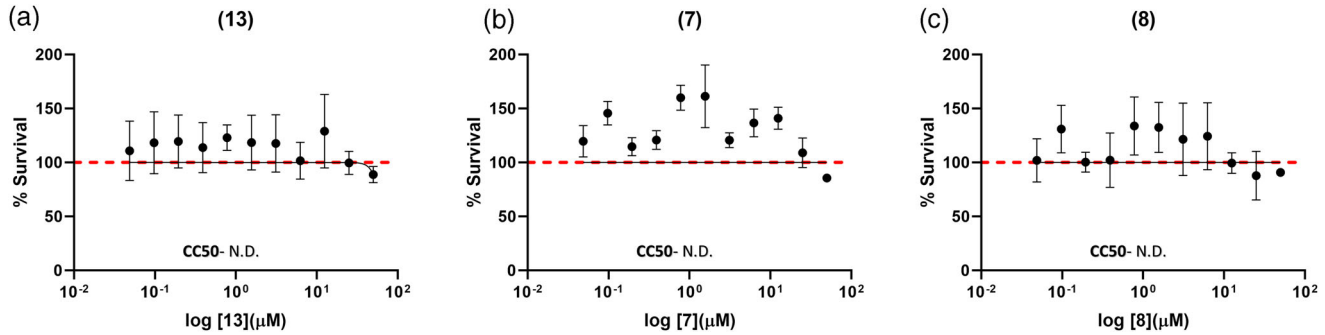

Figure 5. Evaluation of cytotoxicity of synthetic indole compounds in Human Embryonic Kidney (HEK293T) cell line. HEK293T cells were incubated for 72 h with compounds a) (**13**), B) (**7**), and C) (**8**) at concentrations ranging from 0.05 to 50 μM. Cell viability was evaluated using the MTT assay, which measures metabolic activity as an indicator of cell survival. The cytotoxic concentration for 50% cell death (CC_{50}) was determined from the survival curves, which were generated by plotting the percentage of viable cells against the compound concentrations. The graphs represent the survival curves from three independent experiments; each performed in triplicate. Error bars represent the SD. N.D. = Not Determined.

Among the compounds, compound (**8**) demonstrated the most favorable profile, with the highest SI lower-bound estimate (>4.32), suggesting superior antimalarial activity and minimal toxicity to mammalian cells. These findings highlight the selective nature of these hybrid compounds, with (**8**) standing out as the most promising candidate for further investigation. The inability to determine SI values across all three compounds due to a lack of cytotoxicity emphasizes their potential for selective antimalarial action. Minimal impact of these compounds on mammalian cells makes them strong candidates for future therapeutic exploration.

2.5. Gametocidal Activity of Active Compounds Against the Sexual Stages of *P. falciparum*

To investigate the potential of indole-based compounds for transmission-blocking strategies, we evaluated the effects of (**13**), (**7**), and (**8**) on *P. falciparum* gametocytes. Late-stage gametocytes (stages IV and V) expressing luciferase were treated with five serial dilutions of each compound, ranging from 50 to 3.125 μM. Luciferase activity, measured at the end of the assay, served as a proxy for viable gametocytes, with decreased luciferase activity indicating effective gametocyte killing.

As shown in Figure 6, a significant difference in gametocidal efficacy was observed across the compounds. At the highest concentration of 50 μM, (**13**) demonstrated a robust gametocidal effect, reducing luciferase activity by 62.69%, indicative of effective killing of gametocytes. In contrast, both (**7**) and (**8**) exhibited minimal activity, with less than 20% reduction in luciferase activity at their highest concentrations, suggesting negligible or no effect on gametocytes. Primaquine, a well-established gametocidal agent, served as a positive control and exhibited near-complete activity (nearly 100% reduction in luciferase) at a concentration of 10 μM, confirming the assay's validity and reliability.

Interestingly, although (**8**) demonstrated the highest selectivity for the asexual stages of *P. falciparum* in previous assays, it failed to show significant gametocidal activity, indicating that its antimalarial effects are stage-specific and primarily target asexual stages of the parasite's lifecycle. These results suggest that (**13**) holds promise as a transmission-blocking agent and may serve as a valuable scaffold for developing new compounds with enhanced gametocidal activity.

2.6. Triazole Derivatives Mimic and Interfere with Melatonin Action on Parasites

In this experiment, we investigated the potential of triazole-based derivatives to interfere with melatonin-mediated signaling in *P. falciparum*; we tested **16** compounds synthesized using tryptamine and melatonin as base scaffolds. Since melatonin is known to regulate parasite synchronization and proliferation by binding to an uncharacterized receptor and activating the PLC-IP3 signaling cascade, this study aimed to evaluate whether these compounds could mimic or antagonize melatonin's action. Parasites were exposed to the compounds alone and in combination with melatonin to assess their effects on parasitemia. To achieve this end, *P. falciparum* parasites were incubated under the following conditions: 1) 500 nM of each compound alone, 2) 500 nM of each compound combined with 100 nM melatonin, 3) 100 nM melatonin alone (positive control), and 4) DMSO alone (negative control). We performed the assay specifically using a suboptimal compound concentration of 500 nM to determine whether the observed increase in parasitemia was due to compound-mediated activation of melatonin-like signaling or interference with melatonin's effect when co-administered.

Parasitemia was measured to assess the effect of each condition on parasite growth. Statistical analysis was performed using one-way ANOVA with Dunnett's post-hoc test, comparing individual compounds to the negative control, and compounds combined with melatonin to the positive control.

A general trend of increased parasitemia was observed when parasites were incubated with 500 nM of each compound alone (Figure 7). Among the compounds, (**3**) exhibited the most pronounced increase, significantly enhancing parasitemia compared to the DMSO control ($p < 0.001$). (**12**), (**13**), and (**17**) also induced significant increases in parasitemia, albeit to a lesser extent than

Research Article
doi.org/10.1002/slct.202504720

Chemistry Europe
European Chemical Societies Publishing

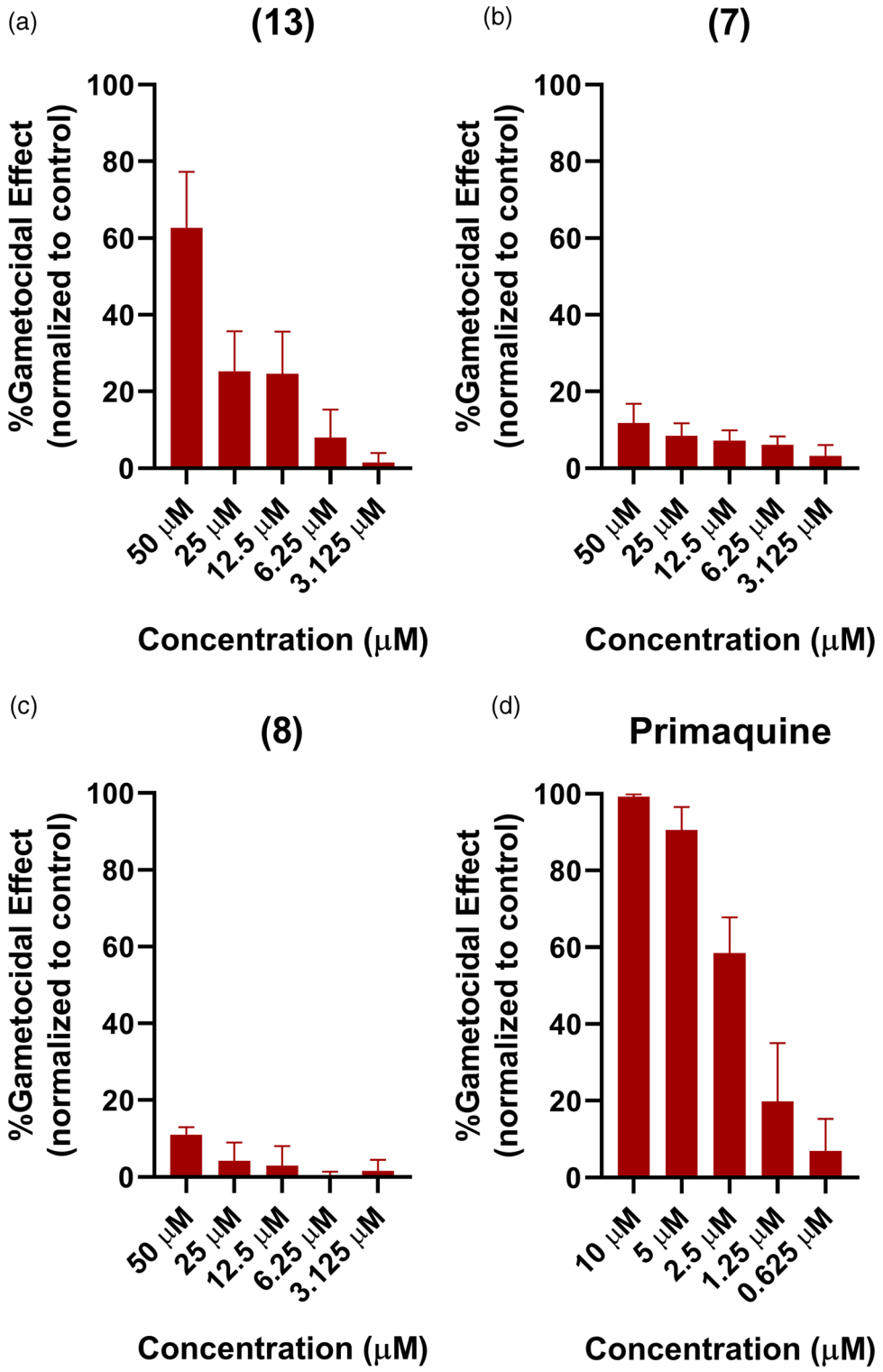

Figure 6. Gametocidal Activity of Indole-Based Compounds Against *P. falciparum* (NF54) Gametocytes. The figure displays the dose-dependent gametocidal effects of three indole-based compounds [(**13**), (**7**), and (**8**)], on late-stage *P. falciparum* gametocytes (stages IV and V). Panels a)–c) show the effects of (**13**), (**7**), and (**8**) on gametocyte viability, measured by luciferase activity and normalized to control. Panel d) represents the effect of the positive control, Primaquine. Compounds were serially diluted in five concentrations ranging from 50 to 3.125 µM. (**13**) exhibited strong gametocidal activity, while (**7**) and (**8**) showed minimal effects at all concentrations tested. Gametocytes were derived from the *P. falciparum* NF54-GFP-Luc line and concentrated using magnetic cell separation (Miltenyi VarioMACS™). They were established at 1% gametocytemia and 2% hematocrit in 96-well plates. After treatment with the compounds, the gametocytes were incubated for 72 h under hypoxic conditions at 37 °C. Luciferase activity, indicative of viable gametocytes, was measured after mixing parasite lysate with luciferin substrate using the Berthold Tristar 5 Multi-Detection System. Error bars indicate the standard deviation (SD) from three independent experiments performed in triplicate.

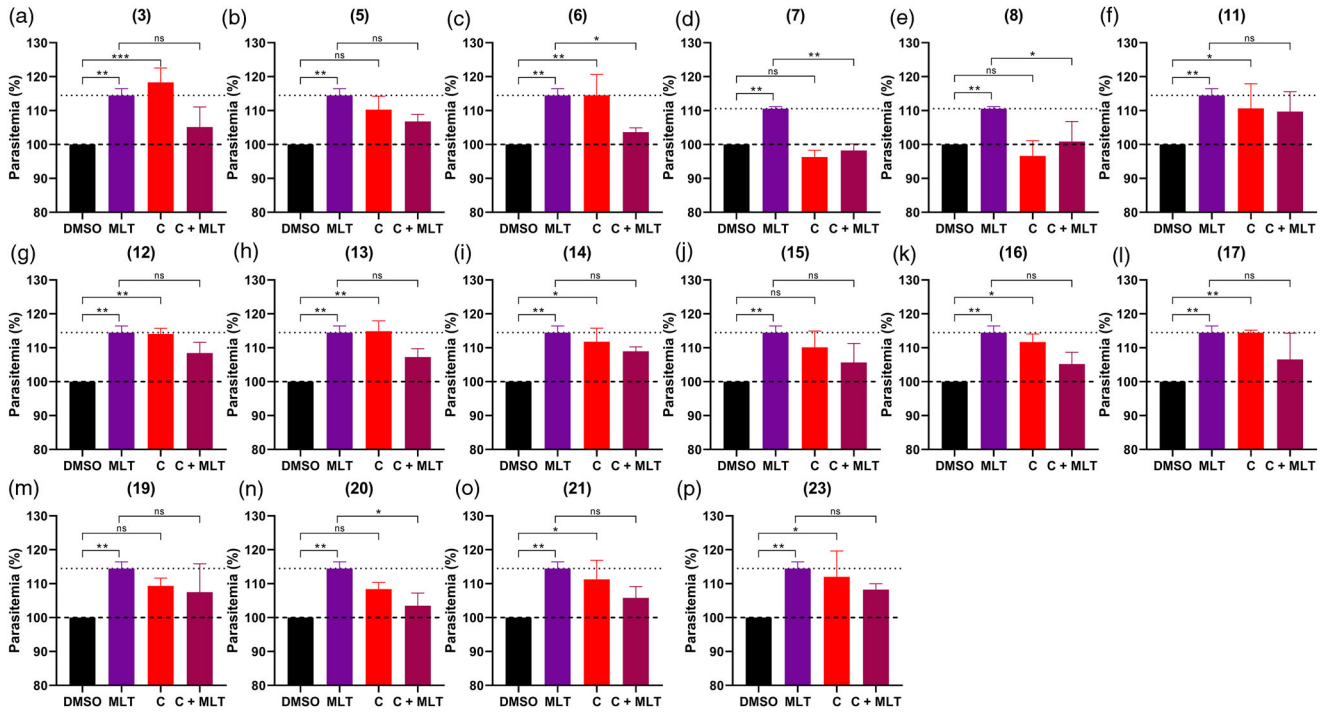

Figure 7. Triazole-based derivatives mimic and compete with melatonin in modulating parasitemia in *P. falciparum*. The bar graphs a)–p) depict parasitemia for the **16** triazole-based compounds: (**3**), (**5**), (**6**), (**7**), (**8**), (**11**), (**12**), (**13**), (**14**), (**15**), (**16**), (**17**), (**19**), (**20**), (**21**), (**23**). Compounds such as (**3**), (**12**), (**13**), and (**17**) significantly increased parasitemia, mimicking melatonin's effect, while (**7**) and (**8**) showed no increase, suggesting no interaction with melatonin pathways. Combined with melatonin (C + MLT), compounds (**7**) and (**8**) strongly inhibited melatonin's effect, reducing parasitemia significantly compared to melatonin alone. Asynchronous *P. falciparum* 3D7 parasites were maintained at 1% parasitemia and 2% hematocrit, treated with compounds (C, 500 nM), melatonin (MLT, 100 nM), or their combination (C + MLT, 500 nM + 100 nM), and incubated for 48 h. Parasitemia was assessed by flow cytometry using SYBR Green I and MitoTracker staining. Parasites treated with DMSO served as the negative control. One-way ANOVA followed by Dunnett's test was used for statistical comparisons, where compounds were tested against the DMSO control, and compound + melatonin conditions were compared to melatonin alone. Error bars represent the standard deviation (SD) from three independent experiments performed in triplicate. Abbreviations: C, compound alone; MLT, melatonin alone; C + MLT, plus melatonin.

Compound (**3**) ($p < 0.01$). These results suggest that these compounds mimic melatonin's action, likely interacting with the same receptor and activating downstream signaling pathways. Conversely, (**7**) and (**8**), which had shown strong antimalarial activity against asexual stages in prior assays, displayed no effect on parasitemia when tested alone. This indicates that their activity is specific to asexual stages and unrelated to melatonin signaling. Other compounds, such as (**14**) and (**20**), induced a modest increase in parasitemia, though these changes were statistically insignificant, suggesting weak interactions with melatonin-related pathways.

When compounds were tested in combination with melatonin (500 nM compound + 100 nM melatonin), distinct competitive effects were observed (Figure 7). (**7**) completely abolished melatonin-induced increases in parasitemia ($p < 0.01$), suggesting strong antagonistic activity. Compounds (**6**), (**8**), and (**20**) also demonstrated strong competitive effects, significantly reducing melatonin's action compared to the melatonin-only control ($p < 0.05$). Other compounds, including (**3**) and (**12**), displayed mild antagonistic effects, reducing melatonin-induced parasitemia to some degree, though these reductions were not statistically significant. The competition observed for these compounds might be partial, reflecting weaker binding affinity or interaction with secondary signaling components.

3. Discussion

Malaria remains a significant global health burden, and the rapid emergence of drug-resistant *P. falciparum* strains underscores the urgent need for novel therapeutic strategies.[26,27] In this study, we synthesized and evaluated a series of derivatives based on melatonin and tryptamine scaffolds, focusing on their anti-plasmodial potential, stage-specific activity, and interaction with melatonin signaling pathways. Our findings highlight the potential of these melatonin-inspired compounds as promising candidates for antimalarial drug development, especially those designed to interfere with melatonin-mediated pathways.

The design strategy for these derivatives focused on modulating lipophilicity by strategically incorporating benzene rings into the core tryptamine and melatonin scaffolds. Additional substituents were introduced onto the aromatic ring to probe their electronic effects and evaluate their capacity to enhance inhibition of *P. falciparum*. In the tryptamine series specifically, a sulfonamide group was selectively incorporated to expand chemical diversity. Unlike melatonin, which already carries bulky and polar functional groups, such as acetamide and methoxyl, the simpler tryptamine scaffold was well-suited to accommodate this moiety without compromising solubility or synthetic feasibility. The introduction of sulfonamide was to explore potential

hydrogen-bonding interactions and to fine-tune polarity, while also building on an earlier study that demonstrated the influence of different functional groups on the melatonin signaling pathway via PfeIK1. The asymmetric design between the two series was therefore intentional, allowing a broader exploration of structure–activity relationships and providing further insight into the role of structural modifications in *Plasmodium* metabolism.

Among the synthesized compounds, compound (**8**) emerged as the most potent against the asexual blood stages of *P. falciparum*, with an IC_{50} of 12 ± 1.9 μM. Electron density donor molecular groups coupled to the resonant structure of the triazole nucleus may be associated with the increased antimalarial activity in (**8**), when compared to (**7**) and (**13**). Compound (**13**), an indole–alkyne precursor, was intentionally included as an indirect precursor of triazoles (**7** and **8**) and a direct precursor of compounds (**14**–**23**). This design allowed us to test whether biological activity arose solely from the triazole ring or if the indolic backbone itself contributed to antiparasitic effects. The measurable activity of (**13**) demonstrates that the indolic-alkynic nucleus makes an intrinsic contribution, likely due to the ability of the terminal acetylene group to interact with diverse biological targets. However, comparison with the triazole derivatives highlights that incorporation of the triazole ring, especially when coupled to a substituted benzene, further modulates and enhances anti-plasmodial activity. This efficacy, coupled with a lack of toxicity toward HEK293T cells, indicates strong parasite-specific activity at a concentration well tolerated by mammalian cells. The other active compounds, (**7**) and (**13**), demonstrated moderate antimalarial activity, suggesting that specific structural modifications in the indole scaffold play a pivotal role in enhancing activity.

Interestingly, compound (**8**), despite its potency against asexual stages, exhibited no significant activity against late-stage gametocytes, indicating stage-specific targeting. Conversely, compound (**13**) demonstrated robust gametocidal activity, reducing luciferase activity by 62.69% at 50 μM, making it a potential candidate for transmission-blocking strategies. Although the gametocytocidal activity we observed is approximately five-fold weaker than that of primaquine, it is notable that primaquine's transmission-blocking efficacy is largely attributed to its 8-aminoquinoline core and a flexible aliphatic side chain, which together balance lipophilicity and basicity to enable efficient membrane permeation and organelle accumulation in gametocytes. In our series, the alkyne moiety functions as a tunable vector. The stage-specific activity observed in these compounds underscores the importance of targeting distinct parasite stages to achieve comprehensive antimalarial effects. Compounds like (**8**), which selectively target asexual stages, could serve as potent partners in combination therapies, while (**13**) holds promise for interrupting parasite transmission. However, future studies could focus on emulating primaquine's transmission-blocking properties by modulating the alkyne substituent to increase lipophilicity within a drug-like window, maintain a basic core, extend the aliphatic chain length, and explore linear, branched, or cycloalkyl termini.

To determine whether the anti-plasmodial effects of the active compounds are mediated through the serpentine receptor 25 (PfSR25), a putative G protein-coupled receptor, we evaluated their efficacy against a PfSR25 knockout strain. The absence of significant differences in IC_{50} values between the wild-type and knockout strains suggests that these compounds exert their effects independently of PfSR25. However, subtle trends, such as slightly increased IC_{50} values for (**13**) and (**8**) and enhanced sensitivity of the knockout strain to (**7**), warrant further exploration of potential indirect interactions with PfSR25-related signaling pathways.

PfSR25 is one of four GPCR-like candidates identified in *P. falciparum*[28] and functions as a potassium (K^+) sensor that mediates intracellular calcium signaling through the PLC-IP3 pathway in response to changes in the concentration of K^+ in the parasites' microenvironment. Beyond signaling, PfSR25 also contributes to parasite survival under stress conditions such as hyperosmotic shock, nutrient deprivation, and oxidative stress.[29] Notably, parasites ablated of PfSR25 show increased sensitivity to antimalarials like lumefantrine and piperaquine, suggesting a broader role in modulating drug susceptibility.[30]

Interestingly, prior studies have demonstrated that chloroquine primarily targets the digestive vacuole and shows similar effects on both wild-type and PfSR25KO strains whereas, lumefantrine displays greater activity against the knockout.[30] Although the precise mechanism of lumefantrine remains unclear, it has been implicated in disrupting heme detoxification,[31] with suggestions that its action may also involve the transporters implicated in resistance like PfMDR1 and PfCRT.[32] The differential response of PfSR25 knockout parasites to lumefantrine supports the hypothesis that PfSR25 may influence how the parasite copes with drug-induced stress, possibly through indirect effects on vacuolar or membrane stability pathways.

Given that previous studies have reported enhanced activity of 1*H*- and 2*H*-1,2,3-triazole-derived compounds against PfSR25-deficient parasites,[33] we were particularly interested in evaluating our own triazole-based compounds in the same model. While our compounds differ in design and complexity from those previously tested, they share a 1,2,3-triazole core, which provided further rationale for examining their activity against the knockout strain. The observed subtle differences in response, especially for (**7**), may reflect structural features that interact with pathways modulated by PfSR25, directly or indirectly. Such findings suggest the potential value of PfSR25 as a modulatory factor in antimalarial efficacy and highlight the importance of considering host-pathogen signaling interactions when exploring the mechanism of action of new compounds.

Melatonin plays a critical role in synchronizing the intraerythrocytic developmental cycle of *P. falciparum* through a signaling cascade involving phospholipase C, inositol triphosphate (IP3), and calcium signaling. The net result of the signalling cascade is observed as increased parasitemia due to coordinated parasite maturation.[6] Previous work by Hotta et al. demonstrated that this effect is most pronounced at 100 nM and is

believed to aid immune evasion by facilitating the simultaneous release of merozoites. This synchronization can be disrupted in vitro by 250nM of luzindole, a melatonin receptor antagonist, confirming the involvement of a melatonin-sensitive signaling pathway. Building on this, our study aimed to identify compounds that could mimic or counteract melatonin's influence on the parasite, potentially revealing new strategies to impair parasite survival or enhance antimalarial efficacy. Using a suboptimal concentration of 500 nM allowed us to detect subtle modulatory effects on melatonin signaling without significant parasite killing. Since luzindole, a known melatonin receptor antagonist, is active only at 250 nM, testing our uncharacterized compounds at 500 nM was appropriate to reveal potential interference with the pathway. This approach helps identify candidates that may enhance combination therapies, even if they lack strong standalone antimalarial activity.

Our results show that several triazole derivatives mimic melatonin's effects, increasing parasitemia when tested alone. Notably, compounds (**3**), (**12**), and (**13**) significantly enhanced parasitemia, suggesting that these compounds may act as melatonin agonists, interacting with the same or related receptors to activate downstream signaling. Interestingly, compound (**13**) stands out as a unique case. While it enhanced parasitemia by modulating the melatonin pathway, it also exhibited a clear antimalarial phenotype. The inhibitory activity of (**13**) appears to arise from interaction with an additional parasite pathway independent of melatonin signaling. The same cannot be said for the other compounds that increased parasitemia, as no corresponding antimalarial activity was detected. Hence, compound (**13**) represents a particularly distinctive and valuable subject for further study. Conversely, compounds (**7**) and (**8**), which lacked agonistic effects, exhibited strong antagonistic activity when tested in combination with melatonin. Compound (**7**) completely abolished melatonin-induced increases in parasitemia, demonstrating potent competitive inhibition. Both compounds also exhibit moderate antimalarial activity with minimal toxicity, positioning them as promising candidates for combination therapy or as scaffolds for further optimization in the development of antimalarial drugs.

These findings reveal a functional diversity in their interaction with melatonin signaling. While some compounds appear to mimic melatonin and enhance parasitemia, others attenuate the melatonin-induced increase, suggesting potential antagonistic activity at the receptor level or interference with downstream signaling. These effects indicate that certain compounds may act as melatonin receptor antagonists, disrupting parasite synchronization and thereby reducing the survival advantage conferred by host-derived melatonin. Our results also fall in line with previous work that demonstrates indole-based compounds to have moderate antimalarial activity, with many of them either blocking or mimicking melatonin activity.[9,24,25] This highlights the potential of the indole class not only as chemical tools to dissect melatonin-mediated pathways in *P. falciparum* but also as promising leads for combination therapies aimed at weakening the parasite's adaptive mechanisms and enhancing susceptibility to antimalarial treatment.

4. Conclusion

The discovery of indole-based compounds that interfere with melatonin signaling marks a significant advancement in developing novel antimalarial agents. These compounds show promise due to their stage-specific activity, low toxicity to mammalian cells, and potential to disrupt parasite synchronization and transmission. Furthermore, their involvement in multiple biological pathways suggests they could complement existing therapies, such as lumefantrine, to enhance efficacy and mitigate the risk of resistance.

We acknowledge that the IC_{50} values obtained in our study fall within the low micromolar range, which is substantially weaker than the potency of established antimalarials. However, these compounds represent first-generation triazole–indole derivatives inspired by melatonin, a molecule that lacks intrinsic anti-plasmodial activity but exhibits clear biological relevance to parasite signaling. In this context, the modest activity observed provides important proof of concept and establishes a foundation for further scaffold optimization. Future efforts should focus on refining the chemical framework to enhance potency and drug-like properties. Strategies may include introducing aliphatic chains onto the triazole ring to tune lipophilicity and interactions within *P. falciparum*, as well as systematically varying electron-donating and electron-withdrawing substituents at different positions of the aromatic core to probe structure–activity relationships. Beyond structural optimization, priority should be given in optimizing the pharmacokinetic and pharmacodynamic profiles of the most promising compounds, including compounds (**8**) and (**13**). Molecular modifications of these candidate prototypes to improve their efficacy, bioavailability, and selectivity for parasite-specific targets will be key to maximizing their therapeutic potential. Investigating the precise molecular targets and signaling pathways involved in their action will provide critical insights into their mechanism and guide the development of next-generation antimalarial agents.

In conclusion, this study highlights the potential of melatonin-inspired compounds as a novel class of antimalarial agents that can target both the asexual and sexual stages of the malaria parasite. These compounds offer a promising strategy for combating drug resistance and enhancing malaria control by modulating melatonin-mediated pathways. This work lays the groundwork for further research into indole-based compounds as versatile tools in the ongoing fight against malaria.

5. Materials and Methods

5.1. Experimental Section

The chemical reagents and solvents used in this study were all of analytical grade and were obtained from Merck AG (Darmstadt, Germany), ACS Científica Química Fina Especializada LTDA (São Paulo, Brazil), and Sciavicco Comércio Indústria LTDA (Belo Horizonte, Brazil). Tryptamine and melatonin were purchased

from Sigma Aldrich Brazil LTDA (São Paulo, Brazil). Melting points were determined using a Quimis device, model 340S, and are reported without correction. Infrared (IR) spectra were recorded using a PerkinElmer FT-IR spectrophotometer, models 1600 Series and Spectrum One, in double-beam mode, on anhydrous potassium bromide pellets or sodium chloride windows, or as films on anhydrous KBr pellets. Absorption values were expressed in wavenumbers (cm^{-1}). The ^{1}H and ^{13}C NMR spectra were obtained in DMSO-d_6 using equipment model Bruker DPX-300 operating at 75 MHz for ^{13}C NMR and 300 MHz for ^{1}H NMR and Bruker Biospin AG 500 MHz for ^{1}H isotopes and 126 MHz for ^{13}C NMR. For all spectra obtained, chemical shifts (δ) were reported in parts per million (ppm) relative to the solvent used. The coupling constant (J) was expressed in Hertz (Hz) and the number of hydrogens was deduced from the relative integral. Reactions were monitored by thin-layer chromatography (TLC) on Merck 60 F254 precoated silica gel plates and visualized under UV light at 254 nm. Column chromatography was performed using a flash silica gel column with an appropriate hexane/ethyl acetate mixture as the eluent. High-resolution mass spectra of the compounds were acquired on an Agilent 6230 mass spectrometer and a Bruker Daltonics micrOTOF-Q II.

5.1.1. Chemistry

General procedure for the synthesis of sulfonamides (10, 11) derived from tryptamine (9): A solution of tryptamine (9) (1.0 mmol, 1.0 equiv.) in dry THF (5 mL) was prepared and cooled to 0 °C. Subsequently, a mixture of p-substituted benzenesulfonyl chloride (1.0 mmol, 1.0 equiv.) and triethylamine (1.2 mmol, 1.2 equiv.) in dry THF (10 mL) was added slowly. The reaction mixture was then warmed to 40–45 °C and stirred for 4 h. Upon completion of the reaction, the formed triethylaminium chloride was removed by filtration, and the solvent was evaporated under reduced pressure. The resulting organic residue was purified by recrystallization from an ethanol/water mixture 1:1 (v/v).

N-(2-(1H-indol-3-yl)ethyl)-4-methylbenzenesulfonamide (10): Obtained in 83.2% yield in the form of white needle-shaped crystals; m.p. 106–108 °C; IR (KBr) ν_{max} (cm^{-1}) 3410 (N–H, indole), 3278 (N–H), 1600 (C═C), 1310, 1150 (S═O); ^{1}H NMR (300 MHz, DMSO-d_6) δ 10.78 (bs, 1H, N–H, indole), 7.65 (d, J = 8.1 Hz, 3H, CH, and CH′, Ar; N–H), 7.31 (dt, J = 12.7, 5.4 Hz, 4H, CH, and CH″, Ar; 2CH, indole), 7.07 (s, 1H, CH), 7.01 (t, J = 7.5 Hz, 1H, CH), 6.91 (t, J = 7.4 Hz, 1H, CH), 2.95 (q, J = 6.5 Hz, 2H, CH_2), 2.75 (t, J = 7.5 Hz, 2H, CH_2), 2.32 (s, 3H, CH_3) ppm; ^{13}C NMR (75 MHz, DMSO-d_6) δ 143.0 (C), 138.1 (C), 136.6 (C), 130.0 (CH), 127.4 (CH), 127.0 (C), 123.4 (CH), 121.4 (CH), 118.7 (CH), 118.4 (CH), 111.8 (C), 111.4 (CH), 43.9 (CH_2), 25.8 (CH_2), 21.4 (CH_3) ppm. HRMS-ESI: Calculated for $C_{17}H_{18}N_2O_2S$ $[M+H]^+$ = 315.1162; Found for $C_{17}H_{18}N_2O_2S$ $[M+H]^+$ = 315.1194

N-(2-(1H-indol-3-yl)ethyl)-4-nitrobenzenesulfonamide (11): Obtained in 76% yield as a shiny brown solid; m.p. 134–136 °C; IR (KBr) ν_{max} (cm^{-1}) 3410 (N–H, indole), 3240 (N–H) 1600 (C═C), 1530, 1325 (NO_2), 1350, 1147 (S═O); ^{1}H NMR (300 MHz, DMSO-d_6) δ 10.78 (bs, 1H, N–H, indole), 8.26 (d, J = 8.9 Hz, 2H, CH, and CH′, Ar), 8.11 (t, J = 5.7 Hz, 1H, N–H), 7.91 (d, J = 8.9 Hz, 2H, CH and CH″, Ar), 7.36 (d, J = 7.7 Hz, 1H, CH), 7.25 (d, J = 8.0 Hz, 1H, CH), 7.09 (d, J = 2.4 Hz, 1H, CH), 7.01 (t, J = 8.2 Hz, 1H, CH), 6.92 (t, J = 7.4 Hz, 1H, CH), 3.12 (q, J = 7.2 Hz, 2H, CH_2), 2.80 (t, J = 7.3 Hz, 2H, CH_2) ppm. ^{13}C NMR (75 MHz, DMSO-d_6) δ 149.6 (C), 146.6 (C), 136.6 (C), 128.1 (CH), 127.3 (C), 124.7 (CH), 123.6 (CH), 121.3 (CH), 118.7 (CH), 118.4 (CH), 111.8 (C), 111.1 (CH), 43.8 (CH_2), 25.8 (CH_2) ppm. HRMS-ESI: Calculated for $C_{16}H_{15}N_3O_4S$ $[M+H]^+$ = 346.0856; Found for $C_{16}H_{15}N_3O_4S$ $[M+H]^+$ = 346.0889

General procedure for the synthesis of the terminal alkyne (3) From melatonin (2): A mixture of melatonin (2) (1.0 mmol, 1.0 equiv.) and sodium hydroxide (1.2 mmol, 1.2 equiv.) in dry DMF (5 mL) was kept at 0 °C under constant stirring for 2 h. Subsequently, an 80% (w/w) solution of propargyl bromide in toluene (2.0 mmol, 2.0 equiv.) was added, and the mixture was stirred for an additional 2 h at room temperature. The reaction was then quenched in water, extracted with ethyl acetate (2 x 20 mL), and washed with brine and water. The organic phase was dried over anhydrous sodium sulfate, filtered, and concentrated under reduced pressure. The crude product was purified by flash column chromatography on silica gel using an ethyl acetate/hexane 7:3 (v/v) elution gradient to obtain the final product.

N-(2-(5-methoxy-1-(prop-2-yn-1-yl)-1H-indol-3 yl)ethyl)acetamide (3): Obtained in 70.3% yield as a yellow solid; m.p. 87–89 °C; IR (KBr) ν_{max} (cm^{-1}) 3280 (N–H, Ac), 3080 (C–H, Ar), 2930 (C–H, Alph), 2120 (C≡C), 1630 (C═O); ^{1}H NMR (500 MHz, DMSO-d_6) δ 7.85 (s, 1H, N–H), 7.35 (d, J = 8.8 Hz, 1H, CH), 7.14 (s, 1H, CH), 7.06 (d, J = 2.4 Hz, 1H, CH), 6.81 (dd, J = 8.8, 2.4 Hz, 1H, CH), 4.95 (d, J = 2.5 Hz, 2H, CH_2), 3.78 (s, 3H, CH_3), 3.32 (s, 1H, CH), 3.27 (q, J = 2.5 Hz, 2H, CH_2), 2.78 (t, J = 7.4 Hz, 2H, CH_2), 1.81 (s, 3H, CH3) ppm. ^{13}C NMR (126 MHz, DMSO-d_6) δ 170.2 (C), 153.9 (C), 131.5 (C), 128.8 (C), 126.8 (CH), 112.4 (CH), 111.8 (C), 111.1 (CH), 101.2 (CH), 80.0 (C), 75.5 (CH), 55.9 (CH3), 39.9 (CH_2), 35.5 (CH_2), 25.4 (CH_2), 23.1 (CH_3). HRMS-ESI: Calculated for $C_{16}H_{18}N_2O_2$ $[M+Na]^+$ = 293.1260; Found for $C_{16}H_{18}N_2O_2$ $[M+Na]^+$ = 293.1263

General procedure for the synthesis of terminal alkynes (12, 13) derived from (10, 11): A solution of (10) or (11) (1.0 mmol, 1.0 equiv.) in dry DMF (10 mL) was mixed with potassium carbonate (1.2 mmol, 1.2 equiv.) and an 80% (w/w) solution of propargyl bromide in toluene (1.2 mmol, 1.2 equiv.). The reaction mixture was stirred continuously for 16 h at room temperature. Upon completion, the mixture was washed with a saturated solution of ammonium chloride and then extracted twice with ethyl acetate (2 x 20 mL). The combined organic phases were washed twice with water and brine, dried over anhydrous sodium sulfate, and concentrated under reduced pressure. The resulting product was recrystallized from a mixture of ethanol and water 3:2 (v/v).

N-(2-(1H-indol-3-yl)ethyl)-4-methyl-N-(prop-2-yn-1-yl) benzenesulfonamide (12): Obtained in 73.5% yield as a shiny white solid; m.p. 115–117 °C; IR (KBr) ν_{max} (cm^{-1}) 3415 (N–H, indole), 2120 (C≡C), 1600 (C═C), 1320, 1150 (S═O); 1H NMR (300

MHz, DMSO-d_6) δ 10.84 (bs, 1H, N–H, indole), 7.65 (d, J = 8.2 Hz, 2H, CH, and CH′, Ar), 7.46 (d, J = 7.7 Hz, 1H, CH), 7.32 (dd, J = 8.1, 4.6 Hz, 3H, CH, and CH″, Ar; CH, indole), 7.15 (s, 1H, CH), 7.03 (t, J = 7.5 Hz, 1H, CH), 6.94 (t, J = 7.4 Hz, 1H, CH), 4.17 (d, J = 2.5 Hz, 2H, CH_2), 3.37–3.33 (m, 2H, CH_2), 3.13 (t, J = 2.2 Hz, 1H, CH), 2.96–2.88 (m, 2H, CH_2), 2.33 (s, 3H, CH_3) ppm. ^{13}C NMR (75 MHz, DMSO-d_6) δ 143.8 (CH), 136.7 (CH), 136.1 (CH), 130.1 (CH), 127.7 (CH), 127.4 (C), 123.5 (CH), 121.5 (CH), 118.8 (CH), 118.5 (CH), 111.9 (CH), 110.9 (CH), 77.9 (C), 76.7 (C), 47.6 (CH_2), 36.8 (CH_2), 24.3 (CH_2), 21.4 (CH_3) ppm. HRMS-ESI: Calculated for $C_{20}H_{20}N_2O_2S$ $[M+H]^+$ = 353.1318; Found for $C_{20}H_{20}N_2O_2S$ $[M+H]^+$ = 353.1357

N-(2-(1H-indol-3-yl)ethyl)-4-nitro-N-(prop-2-yn-1-yl)benzenesulfonamide (13): Obtained in 83.5% yield as a shiny yellow solid; m.p. 173–175 °C; IR (KBr) ν_{max} (cm^{-1}) 3460 (N–H, indole), 3300 (C–H, alkyne), 2120 (C≡C), 1600 (C═C), 1528, 1320 (NO_2), 1343, 1160 (S═O); ^{1}H NMR (300 MHz, DMSO-d_6) δ 10.86 (bs, 1H, N–H, indole), 8.29 (d, J = 8.8 Hz, 2H, CH, and CH′, Ar), 7.99 (d, J = 8.8 Hz, 2H, CH, and CH″, Ar), 7.49 (d, J = 7.7 Hz, 1H, CH), 7.31 (d, J = 8.0 Hz, 1H, CH), 7.24–6.87 (m, 3H, 3CH, indole), 4.6–3.64 (m, 2H, CH_2), 3.49 (t, J = 7.6 Hz, 2H, CH_2), 3.26–3.09 (m, 1H, CH), 2.99 (t, J = 7.6 Hz, 2H, CH2) ppm. ^{13}C NMR (75 MHz, DMSO-d_6) δ 149.7 (C), 144.0 (C), 136.2 (C), 128.7 (CH), 126.8 (C), 124.2 (CH), 123.2 (CH), 121.0 (CH), 118.4 (CH), 118.0 (CH), 111.4 (CH), 110.2 (CH), 77.0 (C), 76.6 (C), 47.2 (CH_2), 36.2 (CH_2), 23.6 (CH_2) ppm. HRMS-ESI: Calculated for $C_{19}H_{17}N_3O_4S$ $[M+H]^+$ = 384.1013; Found for $C_{19}H_{17}N_3O_4S$ $[M+H]^+$ = 384.1052

General procedure for preparing 1H-1,2,3-triazoles derived From melatonin (4–8) and tryptamine (14–23): Copper sulfate pentahydrate (0.5 mmol, 1.0 equiv.) and sodium ascorbate (0.25 mmol, 0.5 equiv.) were sequentially added to a solution containing substituted aryl azides (0.52 mmol, 1.05 equiv.) and either a terminal alkyne derived from tryptamine (12) or (13) (0.5 mmol, 1.0 equiv.), or melatonin (3) (0.5 mmol, 1.0 equiv.) in a mixture of DMF/H2O 1:1 (v/v, 10 mL). The reaction was stirred at room temperature until the starting materials were no longer detectable by TLC. Upon completion, the mixture was extracted with ethyl acetate and water (3 x 20 mL). The combined organic phases were dried over anhydrous sodium sulfate and concentrated under reduced pressure. The crude product was purified by flash column chromatography on silica gel using varying gradients of ethyl acetate and hexane to afford the final product.

N-(2-(5-methoxy-1-((1-(4-nitrophenyl)-1H-1,2,3-triazol-4-yl)methyl)-1H-indol-3-yl)ethyl)acetamide (4): Obtained in 70% yield as a orange solid; m.p. 134–136 °C; IR (KBr) ν_{max} (cm^{-1}) 3270 (N–H, Ac), 3090 (C–H, Ar), 2920 (C–H, Alph), 1630 (C═O), 1520, 1320 (NO_2), 1340, 1220 (C–N, Ar; Alph); 1H NMR (500 MHz, DMSO-d_6) δ 8.90 (s, 1H, CH, triazole), 8.43–8.41 (m, 2H, CH, and CH′, Ar), 8.18–8.15 (m, 2H, CH, and CH″, Ar), 7.97 (t, J = 5.7 Hz, 1H, N–H), 7.46 (d, J = 8.9 Hz, 1H, CH), 7.25 (s, 1H, CH), 7.04 (d, J = 2.4 Hz, 1H, CH), 6.78 (dd, J = 8.9, 2.4 Hz, 1H, CH), 5.46 (s, 2H, CH_2), 3.75 (s, 3H, CH_3), 3.32–3.28 (m, 2H, CH_2), 2.77 (t, J = 7.4 Hz, 2H, CH_2), 1.79 (s, 3H, CH_3) ppm. ^{13}C NMR (126 MHz, DMSO-d_6) δ 167.0 (C), 154.0 (C), 147.3 (C), 146.0 (C), 141.2 (C), 131.8 (C), 128.8 (C), 127.1 (CH), 125.9 (CH), 122.4 (CH), 121.2 (CH), 112.4 (CH), 111.8 (C), 111.1 (CH), 101.5 (CH), 56.1 (CH_3), 41.1 (CH_2), 39.9 (CH_2), 25.5 (CH_2), 23.0 (CH_3) ppm. HRMS-ESI: Calculated for $C_{22}H_{22}N_6O_4$ $[M+Na]^+$ = 457.1594; Found for $C_{22}H_{22}N_6O_4$ $[M+Na]^+$ = 457.1592

N-(2-(1-((1-(4-chlorophenyl)-1H-1,2,3-triazol-4-yl)methyl)-5-methoxy-1H-indol-3-yl)ethyl)acetamide (5): Obtained in 82% yield as a white solid; m.p. 144–146 °C; IR (KBr) ν_{max} (cm^{-1}) 3320 (N–H, Ac), 3090 (C–H, Ar), 2930 (C–H, Alph), 1640 (C═O), 1340, 1220 (C–N, Ar; Alph); ^{1}H NMR (500 MHz, DMSO-d_6) δ 8.73 (s, 1H, CH, triazole), 7.97 (t, J = 5.7 Hz, 1H, N–H), 7.90–7.87 (m, 2H, CH, and CH′, Ar), 7.65–7.63 (m, 2H, CH, and CH″, Ar), 7.46 (d, J = 8.9 Hz, 1H, CH), 7.24 (s, 1H, CH), 7.04 (d, J = 2.4 Hz, 1H, CH), 6.78 (dd, J = 8.8, 2.5 Hz, 1H, CH), 5.43 (s, 2H, CH_2), 3.75 (s, 3H, CH_3), 3.29 (d, J = 5.4 Hz, 2H, CH_2), 2.76 (t, J = 7.4 Hz, 2H, CH_2), 1.79 (s, 3H, CH_3) ppm. $_{13}$C NMR (126 MHz, DMSO-d_6) δ 170.0 (C), 153.9 (C), 145.5 (C), 135.7 (C), 133.5 (C), 131.6 (C), 130.3 (CH), 128.8 (C), 127.1 (CH), 122.3 (CH), 122.1 (CH), 112.2 (CH), 111.7 (C), 111.2 (CH), 101.3 (CH), 55.9 (CH_3), 41.1 (CH_2), 39.9 (CH_2), 25.5 (CH_2), 23.0 (CH_3) ppm. HRMS-ESI: Calculated for $C_{22}H_{22}ClN_5O_2$ $[M+Na]^+$ = 446.1354; Found for $C_{22}H_{22}ClN_5O_2$ $[M+Na]^+$ = 423.1352

N-(2-(1-((1-(4-bromophenyl)-1H-1,2,3-triazol-4-yl)methyl)-5-methoxy-1H-indol-3-yl)ethyl)acetamide (6): Obtained in 91% yield as a white solid; m.p. 156–158 °C; IR (KBr) ν_{max} (cm^{-1}) 3320 (N–H, Ac), 3090 (C–H, Ar), 2920 (C–H Alph), 1640 (C═O), 1340, 1220 (C–N, Ar; Alph), 1070 (C–Br, Ar); ^{1}H NMR (500 MHz, DMSO-d_6) δ 8.68 (s, 1H, CH, triazole), 7.83–7.80 (m, 3H, CH and CH′, Ar; N–H), 7.77–7.74 (m, 2H, CH, and CH″, Ar), 7.44 (d, J = 8.9 Hz, 1H, CH), 7.22 (s, 1H, CH), 7.04 (d, J = 2.4 Hz, 1H, CH), 6.78 (dd, J = 8.8, 2.4 Hz, 1H, CH), 5.42 (s, 2H, CH_2), 3.76 (s, 3H, CH_3), 3.33–3.30 (m, 2H, CH_2), 2.77 (t, J = 7.4 Hz, 2H, CH_2), 1.79 (s, 3H, CH_3) ppm. ^{13}C NMR (126 MHz, DMSO-d_6) δ 169.8 (C), 153.9 (C), 145.5 (C), 136.2 (C), 133.2 (CH), 131.7 (C), 128.8 (C), 127.1 (CH), 122.5 (CH), 122.0 (C), 121.8 (CH), 112.2 (CH), 111.7 (C), 111.2 (CH), 101.3 (CH), 55.9 (CH_3), 41.1 (CH_2), 39.8 (CH_2), 25.5 (CH_2), 23.1 (CH_3) ppm. HRMS-ESI: Calculated for $C_{22}H_{22}BrN_5O_2$ $[M+Na]^+$ = 490.0849; Found for $C_{22}H_{22}BrN_5O_2$ $[M+Na]^+$ = 490.0852

N-(2-(5-methoxy-1-((1-phenyl-1H-1,2,3-triazol-4-yl)methyl)-1H-indol-3-yl)ethyl)acetamide (7): Obtained in 68% yield as a white solid; m.p. 135–137 °C; IR (KBr) ν_{max} (cm^{-1}) 3267 (N–H, Ac), 3080 (C–H, Ar), 2930 (C–H, Alph), 1640 (C═O), 1350, 1225 (C–N, Ar; Alph); ^{1}H NMR (500 MHz, DMSO-d_6) δ 8.65 (s, 1H, CH, triazole), 7.82 (dd, J = 7.6, 1.8 Hz, 3H, CH, and CH′, Ar; N–H), 7.58–7.54 (m, 2H, CH, and CH″, Ar), 7.48–7.44 (m, 2H, CH, Ar; CH, indole), 7.23 (s, 1H, CH), 7.04 (d, J = 2.5 Hz, 1H, CH), 6.78 (dd, J = 8.9, 2.4 Hz, 1H, CH), 5.42 (s, 2H, CH_2), 3.76 (s, 3H, CH_3), 3.39–3.22 (m, 2H, CH_2), 2.78 (d, J = 7.5 Hz, 2H, CH_2), 1.79 (s, 3H, CH_3) ppm. ^{13}C NMR (126 MHz, DMSO-d_6) δ 170.0 (C), 153.9 (C), 145.3 (C), 136.9 (C), 131.7 (C), 130.4 (CH), 129.2 (C), 128.8 (C), 127.1 (CH), 122.0 (CH), 120.6 (CH), 112.2 (CH), 111.7 (C), 111.2 (CH), 101.3 (CH), 55.9 (CH_3), 41.1 (CH_2), 39.9 (CH_2), 25.5 (CH_2), 23.1 (CH_3) ppm. HRMS-ESI: Calculated for $C_{22}H_{23}N_5O_2$ $[M+Na]^+$ = 412.1743; Found for $C_{22}H_{23}N_5O_2$ $[M+Na]^+$ = 412.1745

N-(2-(5-methoxy-1-((1-(4-methoxyphenyl)-1H-1,2,3-triazol-4-yl)methyl)-1H-indol-3-yl)ethyl)acetamide (8): Obtained in 68.1% yield as a white solid; m.p. 124–126 °C; IR (KBr) ν_{max} (cm^{-1}) 3270 (N–H, Ac), 3090 (C–H, Ar), 2940 (C–H Alph), 1630 (C═O), 1345, 1250 (C–N, Ar; Alph), 1020 (C–O); ^{1}H NMR (500 MHz, DMSO-d_6) δ 8.61 (s, 1H, CH, triazole), 7.95 (d, J = 5.6 Hz, 1H, N–H), 7.76–7.73 (m, 2H, CH, and CH′, Ar), 7.47 (d, J = 8.9 Hz, 1H, CH), 7.24 (s, 1H, CH), 7.12–7.09 (m, 2H, CH, and CH″, Ar), 7.04 (d, J = 2.4 Hz, 1H, CH), 6.78 (dd, J = 8.8, 2.4 Hz, 1H, CH), 5.41 (s, 2H, CH_2), 3.81 (s, 3H, CH_3), 3.76 (s, 3H, CH_3), 3.31–3.28 (m, 2H, CH_2), 2.77 (t, J = 7.4 Hz, 2H, CH_2), 1.79 (s, 3H, CH_3) ppm. ^{13}C NMR (126 MHz, DMSO-d_6) δ 170.1 (C), 159.7 (C), 153.8 (C), 145.1 (C), 131.6 (C), 130.3 (C), 128.7 (C), 127.1 (CH), 122.2 (CH), 122.0 (CH), 115.3 (CH), 112.1 (CH), 111.7 (C), 111.2 (CH), 101.1 (CH), 56.0 (CH_3), 55.9 (CH_3), 41.1 (CH_2), 39.9 (CH_2), 25.5 (CH_2), 23.1 (CH_3) ppm. HRMS-ESI: Calculated for $C_{23}H_{25}N_5O_3$ $[M+Na]^+$ = 442.1849; Found for $C_{23}H_{25}N_5O_3$ $[M+Na]^+$ = 442.1852

N-(2-(1H-indol-3-yl)ethyl)-4-methyl-N-((1-(4-nitrophenyl)-1H-1,2,3-triazol-4yl)methyl)benzenesulfonamide (14): Obtained in 82% yield as a light yellow solid; m.p. 167–169 °C; IR (KBr) ν_{max} (cm^{-1}) 3445 (N–H, indole), 3090 (C–H, Ar), 2940 (C–H, Alph), 1600 (C═C), 1520, 1320 (NO_2), 1350, 1150 (S═O); ^{1}H NMR (500 MHz, DMSO-d_6) δ 10.65 (bs, 1H, N–H, indole), 8.57 (s, 1H, CH, triazole), 8.37–8.35 (m, 2H, CH and CH′, Ar), 8.05–8.03 (m, 2H, CH, and CH″, Ar), 7.61 (d, J = 8.2 Hz, 2H, CH, and CH‴, Ar), 7.34 (d, J = 7.9 Hz, 1H, CH), 7.24 (t, J = 8.4 Hz, 3H, CH and CH‴′, Ar; CH, indole), 7.04 (d, J = 2.3 Hz, 1H, CH), 6.96 (t, J = 7.5 Hz, 1H, CH), 6.85 (t, J = 7.4 Hz, 1H, CH), 4.54 (s, 2H, CH_2), 3.44–3.40 (m, 2H, CH_2), 2.90–2.87 (m, 2H, CH_2), 2.23 (s, 3H, CH_3) ppm. ^{13}C NMR (126 MHz, DMSO-d_6) δ 147.1 (C), 144.7 (C), 143.7 (C), 141.0 (C), 136.7 (C), 136.6 (C), 130.2 (CH), 127.4 (CH), 127.3 (C), 126.0 (CH), 123.5 (CH), 123.0 (CH), 121.5 (CH), 121.0 (CH), 118.9 (CH), 118.4 (CH), 111.9 (C), 111.0 (CH), 49.0 (CH_2), 42.7 (CH_2), 24.8 (CH_2), 21.3 (CH_3) ppm. HRMS-ESI: Calculated for $C_{26}H_{24}N_6O_4S$ $[M+Na]^+$ = 539.1471; Found for $C_{26}H_{24}N_6O_4S$ $[M+Na]^+$ = 539.1481

N-(2-(1H-indol-3-yl)ethyl)-N-((1-(4-chlorophenyl)-1H-1,2,3-triazol-4-yl)methyl)-4-methylbenzenesulfonamide (15): Obtained in 83% yield as a white solid; m.p. 172–174 °C; IR (KBr) ν_{max} (cm^{-1}) 3400 (N–H, indole), 3090 (C–H, Ar), 2920 (C–H, Alph), 1590 (C═C), 1340, 1160 (S═O); 1H NMR (500 MHz, DMSO-d_6) 10.74 (bs, 1H, N–H, indole), 8.43 (s, 1H, CH, triazole), 7.83 (d, J = 8.5 Hz, 2H, CH, and CH′, Ar), 7.70–7.65 (m, 4H, CH and CH″; CH, and CH‴, Ar), 7.42 (d, J = 7.7 Hz, 1H, CH), 7.33 (d, J = 7.8 Hz, 3H, CH and CH‴′, Ar; CH, indole), 7.12 (s, 1H, CH), 7.05 (t, J = 7.4 Hz, 1H, CH), 6.94 (t, J = 7.3 Hz, 1H, CH), 4.60 (s, 2H, CH_2), 3.50–3.46 (m, 2H, CH_2), 2.98–2.94 (m, 2H, CH_2), 2.31 (s, 3H, CH_3) ppm. ^{13}C NMR (126 MHz, DMSO-d_6) δ 144.1 (C), 143.7 (C), 136.8 (C), 136.6 (C), 135.6 (C), 133.5 (C), 130.3(CH), 130.2 (CH), 127.4 (CH), 127.3 (C), 123.5 (CH), 122.6 (CH), 122.1 (CH), 121.5 (CH), 118.9 (CH), 118.5 (CH), 111.9 (C), 111.0 (CH), 48.8 (CH_2), 42.7 (CH_2), 24.8 (CH_2), 21.3 (CH_3) ppm. HRMS-ESI: Calculated for $C_{26}H_{24}ClN_5O_2S$ $[M+H]^+$ = 506.1412; Found for $C_{26}H_{24}ClN_5O_2S$ $[M+H]^+$ = 506.1454

N-(2-(1H-indol-3-yl)ethyl)-N-((1-(4-bromophenyl)-1H-1,2,3-triazol-4-yl)methyl)-4-methylbenzenesulfonamide (16): Obtained in 87% yield as a white solid; m.p. 170–173 °C; IR (KBr) ν_{max} (cm^{-1}) 3400 (N–H, indole), 3090 (C–H, Ar), 2920 (C–H, Alph), 1590 (C═C), 1335, 1150 (S═O); ^{1}H NMR (500 MHz, DMSO-d_6) δ 10.79 (bs, 1H, N–H, indole), 8.47 (s, 1H, CH, triazole), 7.74 (s, 4H, CH and CH′; CH and CH″, Ar), 7.64 (d, J = 7.9 Hz, 2H, CH and CH‴, Ar), 7.38 (d, J = 7.9 Hz, 1H, CH), 7.27 (d, J = 7.9 Hz, 3H, CH and CH‴′, Ar; CH, indole), 7.10 (s, 1H, CH), 7.00 (t, J = 7.6 Hz, 1H, CH), 6.89 (t, J = 7.5 Hz, 1H, CH), 4.56 (s, 2H, CH_2), 3.42 (t, J = 8.0 Hz, 2H, CH_2), 2.90 (t, J = 8.0 Hz, 2H, CH_2), 2.25 (s, 3H, CH_3) ppm. ^{13}C NMR (126 MHz, DMSO-d_6) δ 144.2 (C), 143.6 (C), 136.9 (C), 136.6 (C), 136.1 (C), 133.2 (CH), 130.1 (CH), 127.4 (CH), 127.3 (C), 123.5 (CH), 122.6 (CH), 122.3 (CH), 121.7 (CH), 121.4 (CH), 118.8 (CH), 118.5 (CH), 111.9 (C), 111.0 (CH), 48.8 (CH_2), 42.7 (CH_2), 24.9 (CH_2), 21.3 (CH_3) ppm. HRMS-ESI: Calculated for $C_{26}H_{24}BrN_5O_2S$ $[M+H]^+$ = 550.0907; Found for $C_{26}H_{24}BrN_5O_2S$ $[M+H]^+$ = 550.0948

N-(2-(1H-indol-3-yl)ethyl)-4-methyl-N-((1-phenyl-1H-1,2,3-triazol-4-yl)methyl) benzenesulfonamide (17): Obtained in 82% yield as a light yellow solid; m.p. 44–47 °C; IR (KBr) ν_{max} (cm^{-1}) 3400 (N–H, indole), 3060 (C–H, Ar), 2920 (C–H, Alph), 1590 (C═C), 1335, 1150 (S═O); ^{1}H NMR (300 MHz, DMSO-d_6) δ 10.73 (bs, 1H, N–H, indole), 8.36 (s, 1H, CH, triazole), 7.77 (d, J = 7.8 Hz, 2H, CH and CH′, Ar), 7.68 (d, J = 8.2 Hz, 2H, CH and CH″, Ar), 7.59 (t, J = 7.8 Hz, 3H, CH and CH‴; CH, Ar), 7.49 (t, J = 7.4 Hz, 1H, CH), 7.42 (d, J = 7.9 Hz, 1H, CH), 7.33–7.31 (m, 2H, CH and CH‴′, Ar), 7.12 (d, J = 2.1 Hz, 1H, CH), 7.04 (t, J = 7.3 Hz, 1H, CH), 6.93 (t, J = 7.3 Hz, 1H, CH), 4.60 (s, 2H, CH_2), 3.49–3.46 (m, 2H, CH_2), 2.97–2.94 (m, 2H, CH_2), 2.30 (s, 3H, CH_3) ppm. ^{13}C NMR (126 MHz, DMSO-d_6) δ 143.9 (C), 143.7 (C), 136.8 (C), 136.6 (C), 130.4 (CH), 130.2 (CH), 129.2 (CH), 127.4 (CH), 127.3 (C), 123.5 (CH), 122.5 (CH), 121.5 (CH), 120.4 (CH), 118.9 (CH), 118.5 (CH), 111.9 (C), 111.1 (CH), 48.7 (CH_2), 42.6 (CH_2), 24.8 (CH_2), 21.3 (CH_3) ppm. HRMS-ESI: Calculated for $C_{26}H_{25}N_5O_2S$ $[M+H]^+$ = 472.1802; Found for $C_{26}H_{25}N_5O_2S$ $[M+H]^+$ = 472.1848

N-(2-(1H-indol-3-yl)ethyl)-N-((1-(4-methoxyphenyl)-1H-1,2,3-triazol-4-yl)methyl)-4-methylbenzenesulfonamide (18): Obtained in 91% yield as a white solid; m.p. 118–120 °C; IR (KBr) ν_{max} (cm^{-1}) 3400 (N–H, indole), 3090 (C–H, Ar), 2920 (C–H, Alph), 1600 (C═C), 1335, 1156 (S═O), 1000 (C–O); ^{1}H NMR (500 MHz, DMSO-d6) δ 10.74 (bs, 1H, N–H, indole), 8.27 (s, 1H, CH, triazole), 7.69–7.66 (m, 4H, CH and CH′; CH and CH″, Ar), 7.42 (d, J = 8.2 Hz, 1H, CH), 7.33 (dd, J = 8.1, 4.3 Hz, 3H, CH and CH‴, Ar; CH, indole), 7.13 (d, J = 9.0 Hz, 3H, CH and CH‴′, Ar; CH, indole), 7.05 (t, J = 7.5 Hz, 1H, CH), 6, 94 (t, J = 7.4 Hz, 1H, CH), 4.59 (s, 2H, CH_2), 3.84 (s, 3H, CH_3), 3.48–3.45 (m, 2H, CH_2), 2.97–2.93 (m, 2H, CH_2), 2.33 (s, 3H, CH_3) ppm. ^{13}C NMR (126 MHz, DMSO-d_6) δ 159.7 (C), 143.7 (C), 143.6 (C), 136.8 (C), 136.6 (C), 130.3 (C), 130.2 (CH), 127.4 (CH), 127.3 (C), 123.5 (CH), 122.5 (CH), 122.1 (CH), 121.5 (CH), 118.9 (CH), 118.5 (CH), 115.3 (CH), 111.9 (C), 111.1 (CH), 56.0 (CH_3), 48.7 (CH_2), 42.6 (CH_2), 24.8 (CH_2), 21.3 (CH_3) ppm. HRMS-ESI: Calculated for $C_{27}H_{27}N_5O_3S$ $[M+Na]^+$ = 524.1726; Found for $C_{27}H_{27}N_5O_3S$ $[M+Na]^+$ = 524.1726

N-(2-(1H-indol-3-yl)ethyl)-4-nitro-N-((1-(4-nitrophenyl)-1H-1,2,3-triazol-4-yl)methyl)benzenesulfonamide (19): Obtained in 83% yield as a orange solid; m.p. 165–168 °C; IR (KBr) ν_{max} (cm^{-1}) 3410

(N–H, indole), 3090 (C–H, Ar), 2930 (C–H, Alph), 1600 (C═C), 1520, 1320 (NO2), 1330, 1150 (S═O); ^{1}H NMR (300 MHz, DMSO-d_6) δ 10.79 (bs, 1H, N–H, indole), 8.85 (s, 1H, CH, triazole), 8.40 (d, J = 9.0 Hz, 2H, CH and CH′, Ar), 8.14 (t, J = 8.4 Hz, 4H, CH and CH″; CH and CH‴, Ar), 7.91 (d, J = 8.7 Hz, 2H, CH and CH‴′, Ar), 7.38 (d, J = 7.7 Hz, 1H, CH), 7.22 (d, J = 8.0 Hz, 1H, CH), 7.10 (s, 1H, CH), 6.97 (t, J = 7.5 Hz, 1H, CH), 6.87 (t, J = 7.3 Hz, 1H, CH), 4.71 (s, 2H, CH_2), 3.53 (t, J = 7.3 Hz, 2H, CH_2), 2.95 (t, J = 7.3 Hz, 2H, CH_2) ppm. ^{13}C NMR (75 MHz, DMSO-d_6) δ 149.8 (C), 147.2 (C), 145.3 (C), 144.4 (C), 141.1 (C), 136.6 (C), 128.7 (CH), 127.3 (C), 126.0 (CH), 124.6 (CH), 123.7 (CH), 123.2 (CH), 121.4 (CH), 121.0 (CH), 118.8 (CH), 118.5 (CH), 111.8 (C), 110.7 (CH), 48.7 (CH_2), 42.3 (CH_2), 24.5 (CH_2) ppm. HRMS-ESI: Calculated for $C_{25}H_{21}N_7O_6S$ $[M+Na]^+$ = 570.1166; Found for $C_{25}H_{21}N_7O_6S$ $[M+Na]^+$ = 570.1179

N-(2-(1H-indol-3-yl)ethyl)-N-((1-(4-chlorophenyl)-1H-1,2,3-triazol-4-yl)methyl)-4-nitrobenzenesulfonamide (20): Obtained in 76.5% yield as a orange solid; m.p. 156–158 °C; IR (KBr) ν_{max} (cm^{-1}) 3410 (N–H, indole), 3100 (C–H, Ar), 2920 (C–H, Alph), 1600 (C═C), 1520, 1320 (NO_2), 1330, 1160 (S═O); ^{1}H NMR (300 MHz, DMSO-d_6) δ 10.80 (bs, 1H, N–H, indole), 8.65 (s, 1H, CH, triazole), 8.14 (d, J = 8.5 Hz, 2H, CH and CH′, Ar), 7.86 (dd, J = 18.7, 8.4 Hz, 4H, CH and CH″; CH and CH‴, Ar), 7.61 (d, J = 8.4 Hz, 2H, CH and CH‴′, Ar), 7.38 (d, J = 7.9 Hz, 1H, CH), 7.23 (d, J = 8.1 Hz, 1H, CH), 7.10 (s, 1H, CH), 6.93 (dt, J = 31.2, 7.3 Hz, 2H, 2CH, indole), 4.68 (s, 2H, CH_2), 3.52 (t, J = 7.5 Hz, 2H, CH_2), 2.94 (t, J = 7.6 Hz, 2H, CH_2) ppm. ^{13}C NMR (75 MHz, DMSO-d_6) δ 149.7 (C), 145.3 (C), 143.8 (C), 136.6 (C), 135.6 (C), 133.4 (C), 130.3 (CH), 128.7 (CH), 127.3 (C), 124.6 (CH), 123.7 (CH), 122.8 (CH), 122.1 (CH), 121.4 (CH), 118.8 (CH), 118.5 (CH), 111.8 (C), 110.7 (CH), 48.6 (CH_2), 42.3 (CH_2), 24.5 (CH_2) ppm. HRMS-ESI: Calculated for $C_{25}H_{21}ClN_6O_4S$ $[M+H]^+$ = 537.1106; Found for $C_{25}H_{21}ClN_6O_4S$ $[M+H]^+$ = 537.1148

N-(2-(1H-indol-3-yl)ethyl)-N-((1-(4-bromophenyl)-1H-1,2,3-triazol-4-yl)methyl)-4-nitrobenzenesulfonamide (21): Obtained in 76% yield as a orange solid; m.p. 160–162 °C; IR (KBr) ν_{max} (cm-1) 3425 (N–H, indole), 3100 (C–H, Ar), 2930 (C–H, Alph), 1600 (C═C), 1525, 1320 (NO_2), 1350, 1160 (S═O); ^{1}H NMR (500 MHz, DMSO-d_6) δ 10.81 (bs, 1H, N–H, indole), 8.65 (s, 1H, CH, triazole), 8.20–8.18 (m, 2H, CH and CH′, Ar), 7.94–7.92 (m, 2H, CH and CH″, Ar), 7.80–7.78 (m, 4H, CH and CH‴; CH and CH‴′, Ar), 7.42 (d, J = 7.9 Hz, 1H, CH), 7.27 (d, J = 8.1 Hz, 1H, CH), 7.13 (d, J = 2.3 Hz, 1H, CH), 7.04–7.01 (m, 1H, CH), 6.94–6.90 (m, 1H, CH), 4.71 (s, 2H, CH_2), 3.57 (d, J = 1.5 Hz, 2H, CH_2), 3.01–2.96 (m, 2H, CH_2) ppm. ^{13}C NMR (75 MHz, DMSO-d6) δ 149.8 (C), 145.3 (C), 143.9 (C), 136.6 (C), 136.0 (C), 133.2 (C), 128.7 (CH), 127.3 (C), 124.6 (CH), 123.7 (CH), 122.8 (CH), 122.3 (CH), 121.9 (CH), 121.4 (CH), 118.8 (CH), 118.5 (CH), 111.9 (C), 110.8 (CH), 48.7 (CH_2), 42.3 (CH_2), 24.5 (CH_2) ppm. HRMS-ESI: Calculated for $C_{25}H_{21}BrN_6O_4S$ $[M+Na]^+$ = 603.0420; Found for $C_{25}H_{21}BrN_6O_4S$ $[M+Na]^+$ = 603.0424

N-(2-(1H-indol-3-yl)ethyl)-4-nitro-N-((1-phenyl-1H-1,2,3-triazol-4yl)methyl)benzenesulfonamide (22): Obtained in 59.4% yield as a orange solid; m.p. 139–141 °C; IR (KBr) ν_{max} (cm^{-1}) 3415 (N–H, indole), 3060 (C–H, Ar), 2920 (C–H, Alph), 1600 (C═C), 1525, 1320 (NO_2), 1350, 1160 (S═O); ^{1}H NMR (300 MHz, DMSO-d_6) δ 10.80 (bs, 1H, N–H, indole), 8.60 (s, 1H, CH, triazole), 8.16 (d, J = 9.0 Hz, 2H, CH and CH′, Ar), 7.91 (d, J = 8.9 Hz, 2H, CH and CH″, Ar), 7.77 (d, J = 7.9 Hz, 2H, CH and CH‴, Ar), 7.56–7.50 (m, 2H, CH and CH‴′, Ar), 7.43 (dd, J = 18.8, 7.8 Hz, 2H, CH, Ar; CH, indole), 7.24 (d, J = 8.0 Hz, 1H, CH), 7.11 (d, J = 2.4 Hz, 1H, CH), 6.99 (t, J = 7.7 Hz, 1H, CH), 6.88 (t, J = 7.4 Hz, 1H, CH), 4.69 (s, 2H, CH_2), 3.64–3.47 (m, 2H, CH_2), 3.07–2.85 (m, 2H, CH_2) ppm. ^{1}3C NMR (75 MHz, DMSO-d_6) δ 149.8 (C), 145.4 (C), 143.5 (C), 136.8 (C), 136.6 (C), 130.3 (CH), 129.2 (CH), 128.7 (CH), 127.3 (C), 124.6 (CH), 123.6 (CH), 122.7 (CH), 121.4 (CH), 120.4 (CH), 118.8 (CH), 118.5 (CH), 111.8 (C), 110.8 (CH), 48.6 (CH_2), 42.3 (CH_2), 24.6 (CH_2) ppm. HRMS-ESI: Calculated for $C_{25}H_{22}N_6O_4S$ $[M+H]^+$ = 503.1496; Found for $C_{25}H_{22}N_6O_4S$ $[M+H]^+$ = 503.1538

N-(2-(1H-indol-3-yl)ethyl)-N-((1-(4-methoxyphenyl)-1H-1,2,3-triazol-4-yl)methyl)-4-nitrobenzenesulfonamide (23): Obtained in 72% yield as a yellow solid; m.p. 115–117 °C; IR (KBr) ν_{max} (cm^{-1}) 3410 (N–H, indole), 3100 (C–H, Ar), 2920 (C–H, Alph), 1600 (C═C), 1520, 1320 (NO2), 1350, 1150 (S═O), 1020 (C–O); ^{1}H NMR (300 MHz, DMSO-d_6) δ 10.81 (bs, 1H, N–H, indole), 8.51 (s, 1H, CH, triazole), 8.15 (d, J = 8.5 Hz, 2H, CH and CH′, Ar), 7.90 (d, J = 8.5 Hz, 2H, CH, and CH″, Ar), 7.67 (d, J = 8.7 Hz, 2H, CH, and CH‴, Ar), 7.38 (d, J = 7.7 Hz, 1H, CH), 7.23 (d, J = 8.0 Hz, 1H, CH), 7.11–7.04 (m, 3H, CH and CH‴′, Ar; CH, indole), 6.99 (t, J = 7.4 Hz, 1H, CH), 6.88 (t, J = 7.3 Hz, 1H, CH), 4.67 (s, 2H, CH_2), 3.78 (s, 3H, CH_3), 3.56–3.48 (m, 2H, CH_2), 2.99–2.89 (m, 2H, CH_2) ppm. ^{13}C NMR (75 MHz, DMSO-d_6) δ 159.7 (C), 149.7 (C), 145.3 (C), 143.3 (C), 136.6 (C), 130.2 (C), 128.7 (CH), 127.3 (C), 124.6 (CH), 123.6 (CH), 122.7 (CH), 122.1 (CH), 121.4 (CH), 118.8 (CH), 118.5 (CH), 115.3 (CH), 111.8 (C), 110.7 (CH), 56.0 (CH_3), 48.5 (CH_2), 42.3 (CH_2), 24.5 (CH_2) ppm. HRMS-ESI: Calculated for $C_{26}H_{24}N_6O_5S$ $[M+H]^+$ = 533.1602; Found for $C_{26}H_{24}N_6O_5S$ $[M+H]^+$ = 533.1648

5.1.2. Culture of P. falciparum

The *P. falciparum* strains 3D7 and SR25KO were cultured at 37 °C in RPMI-1640 medium (Gibco, Waltham, MA, USA), supplemented with 0.21% sodium bicarbonate (Sigma, Burlington, MA, USA) and 50 mg.L-1 hypoxanthine (Sigma). This culture medium was enriched with 0.5% AlbuMAX I (Gibco) and maintained under controlled atmospheric conditions with 5% CO_2, 5% O_2, and 90% N_2. The cultures were refreshed daily with fresh complete medium, and rapid-stained blood smears (Panotico stain) were prepared to assess parasite growth and morphology.

5.1.3. Drug Susceptibility Testing in P. falciparum

To study how synthetic compounds, impact the intraerythrocytic stages of *P. falciparum*, we used a flow cytometry-based assay to measure parasitemia. An initial parasitemia level of 0.3% and 1% hematocrit were set for the assay, and cultures were exposed to varying concentrations of each compound, from 0.1 to 100 µM, over a 72-h period. For staining, SYBR Green I (SG-I; Invitrogen, Waltham, MA, USA) targeted nucleic acids, while MitoTracker Deep Red (MT-Red; Invitrogen) labeled the mitochondria, allowing for detailed cytometric analysis. Around 10,000 cells were

analyzed per sample using an Accuri C6 flow cytometer (Becton Dickinson, San Jose, CA, USA) and FlowJo software. Dot plots (side scatter versus fluorescence) facilitated the determination of parasitemia. Parasites treated with 0.125% DMSO served as negative controls to establish baseline responses.

5.1.4. Cytotoxicity Assay in HEK293T Cells

Human embryonic kidney (HEK293T) cells were cultured in vented 75 cm^2 flasks (Greiner Bio-One, Frickenhausen, Germany) under humidified conditions at 37 °C with 5% CO_2, using Dulbecco's Modified Eagle Medium (DMEM; Gibco) supplemented with 10% fetal bovine serum, 100 U/mL penicillin, and 100 µg/mL streptomycin (Sigma). To assess cytotoxicity, we employed the MTT assay,[23,24] which measures cell viability and proliferation. Cells (10^4 per well) were plated in 96-well plates and exposed to compounds at concentrations from 0.1 to 100 µM for 72 h. Following this incubation, the MTT reagent was added for 3 h, and absorbance was recorded at 570 nm using the FlexStation 3 Multi-Mode Microplate Reader (Molecular Devices, Sunnyvale, CA, USA). Controls included DMSO (0.13%) as a negative control and digitonin as a positive control to validate assay specificity. The selectivity index (SI) for each compound was calculated as the ratio of the CC_{50} (cytotoxic concentration for 50% cell viability) to IC_{50} (inhibitory concentration for 50% reduction in parasitemia) values, to assess whether the compounds exhibited higher toxicity to *P. falciparum* or the host cells (HEK293T).

5.1.5. Evaluation of Indole Derivatives on Gametocyte Stages of P. falciparum

Gametocytes derived from *P. falciparum* NF54-GFP-Luc line were established at 1% gametocytemia and 2% hematocrit for the assay in 96-well plates. Gametocytes were then treated with various test compounds, dissolved in DMSO, and incubated under hypoxic conditions at 37 °C for 72 h. Following incubation, luciferase activity in the gametocytes was quantified. For this assay, the parasite lysate was created by following the manufacturer's protocol, and 20 µL of this lysate was mixed with 20 µL of luciferin substrate (Promega Luciferase Assay System) at room temperature, and bioluminescence was measured over a 10-s integration period using the Berthold Tristar 5 Multi-Detection System.

5.1.6. Evaluation of Indole Derivatives on P. falciparum Parasitemia

To investigate the impact of indole derivatives on *P. falciparum* parasitemia, we treated 1% 3D7 cultures at 2% hematocrit with 500 nM of 1*H*-1,2,3-triazole and benzene ring derivatives for 48 h. Melatonin (100 nM) served as a positive control, while DMSO (0.0013% v/v) acted as the negative control. The DMSO concentration was matched to the level present in the compound solutions at 500 nM. Parasite activity and parasitemia were assessed using SG-I and MT-Red staining, with the data normalized against DMSO-treated controls. Furthermore, we evaluated the potential of indole compounds to interfere with melatonin's effects on parasitemia by incubating 3D7 parasites with 500 nM indole derivatives alongside 100 nM melatonin for 48 h.

Acknowledgments

The authors extend our gratitude to COLSAN (São Paulo, Brazil) for providing the blood used in parasite culturing and experimental procedures. All human biological samples were ethically sourced, and their use in research complied with informed consent guidelines under an IRB/EC-approved protocol. This study was approved by the Research Ethics Committee of the Faculty of Pharmaceutical Sciences, University of São Paulo (FCF-USP), under the identification number CAAE 46598621.2.0000.0067. This work was supported by a grant from the São Paulo Research Foundation (FAPESP) awarded to CRSG (Process 2017/08684–7). AM is a recipient of a CAPES fellowship (88887.896791/2023-00). The funders had no role in study design, data collection and analysis, decision to publish, or manuscript preparation.

The Article Processing Charge for the publication of this research was funded by the Coordenacao de Aperfeicoamento de Pessoal de Nivel Superior - Brasil (CAPES) (ROR identifier: 00x0ma614).

Conflict of Interests

The authors declare no conflict of interest.

Data Availability Statement

The data that support the findings of this study are available from the corresponding author upon reasonable request.

Keywords: Antimalarials · Click chemistry · Indole derivatives · Melatonin signaling · *Plasmodium falciparum*

[1] WHO Organization, World Malaria Report 2023, World Health Organization, **2023**.
[2] E. G. Tse, M. Korsik, M. H. Todd, *Malar. J.* **2019**, *18*, 93, https://doi.org/10.1186/s12936-019-2724-z.
[3] A. Uddin, M. Chawla, I. Irfan, S. Mahajan, S. Singh, M. Abid, *RSC Med. Chem.* **2021**, *12*, 24–42, https://doi.org/10.1039/D0MD00244E.
[4] E. Cecon, L. Liu, R. Jockers, *J. Pineal Res.* **2019**, *67*, e12606, https://doi.org/10.1111/jpi.12606.
[5] B. Claustrat, J. Leston, *Neurochirurgie* **2015**, *61*, 77–84, https://doi.org/10.1016/j.neuchi.2015.03.002.
[6] C. T. Hotta, M. L. Gazarini, F. H. Beraldo, F. P. Varotti, C. Lopes, R. P. Markus, T. Pozzan, C. R. Garcia, *Nat. Cell Biol.* **2000**, *2*, 466–468, https://doi.org/10.1038/35017112.
[7] P. Bagnaresi, E. Alves, H. Borges da Silva, S. Epiphanio, M. M. Mota, C. R. Garcia, *Int. J. Gen. Med.* **2009**, 47–55.
[8] F. H. Beraldo, F. M. Almeida, A. M. da Silva, C. R. Garcia, *J. Cell Biol.* **2005**, *170*, 551–557, https://doi.org/10.1083/jcb.200505117.
[9] D. C. Schuck, A. K. Jordão, M. Nakabashi, A. C. Cunha, V. F. Ferreira, C. R. S. Garcia, *Eur. J. Med. Chem.* **2014**, *78*, 375–382, https://doi.org/10.1016/j.ejmech.2014.03.055.
[10] A. Budu, R. Peres, V. B. Bueno, L. H. Catalani, C. R. Garcia, *J. Pineal Res.* **2007**, *42*, 261–266, https://doi.org/10.1111/j.1600-079X.2006.00414.x.

[11] P.-E. Campos, E. Pichon, C. Moriou, P. Clerc, R. Trépos, M. Frederich, N. De Voogd, C. Hellio, A. Gauvin-Bialecki, A. Al-Mourabit, *Mar. Drugs* **2019**, *17*, 167, https://doi.org/10.3390/md17030167.
[12] W. Furuyama, M. Enomoto, E. Mossaad, S. Kawai, K. Mikoshiba, S. Kawazu, *Biochem. Biophys. Res. Commun.* **2014**, *446*, 125–131, https://doi.org/10.1016/j.bbrc.2014.02.070.
[13] T. Luthra, A. K. Nayak, S. Bose, S. Chakrabarti, A. Gupta, S. Sen, *Eur. J. Med. Chem.* **2019**, *168*, 11–27, https://doi.org/10.1016/j.ejmech.2019.02.019.
[14] L. S. Fernandez, M. S. Buchanan, A. R. Carroll, Y. J. Feng, R. J. Quinn, V. M. Avery, *Org. Lett.* **2009**, *11*, 329–332, https://doi.org/10.1021/ol802506n.
[15] L. S. Fernandez, M. L. Sykes, K. T. Andrews, V. M. Avery, *Int. J. Antimicrob. Agents* **2010**, *36*, 275–279, https://doi.org/10.1016/j.ijantimicag.2010.05.008.
[16] H. Turner, *Future Med. Chem.* **2016**, *8*, 227–238, https://doi.org/10.4155/fmc.15.177.
[17] C. V. Plowe, *Malar. J.* **2022**, *21*, 104, https://doi.org/10.1186/s12936-022-04115-8.
[18] H. C. Kolb, M. Finn, K. B. Sharpless, *Angew. Chem., Int. Ed.* **2001**, *40*, 2004–2021, https://doi.org/10.1002/1521-3773(20010601)40:11%3c2004::AID-ANIE2004%3e3.0.CO;2-5.
[19] V. V. Rostovtsev, L. G. Green, V. V. Fokin, K. B. Sharpless, *J. Am. Chem. Soc.* **2002**, *124*, 2708–2711.
[20] N. Devender, S. Gunjan, R. Tripathi, R. P. Tripathi, *Eur. J. Med. Chem.* **2017**, *131*, 171–184, https://doi.org/10.1016/j.ejmech.2017.03.010.
[21] G. Poje, L. Pessanha De Carvalho, J. Held, D. Moita, M. Prudêncio, I. Perković, T. Tandarić, R. Vianello, Z. Rajić, *Eur. J. Med. Chem.* **2022**, *238*, 114408, https://doi.org/10.1016/j.ejmech.2022.114408.
[22] G. Poje, M. Marinović, K. Pavić, M. Mioč, M. Kralj, L. P. De Carvalho, J. Held, I. Perković, Z. Rajić, *Int. J. Mol. Sci.* **2022**, *23*, 9315, https://doi.org/10.3390/ijms23169315.
[23] V. Garg, R. K. Maurya, P. V. Thanikachalam, G. Bansal, V. Monga, *Eur. J. Med. Chem.* **2019**, *180*, 562–612.
[24] B. K. M. Dias, M. Nakabashi, M. R. R. Alves, D. P. Portella, B. M. Dos Santos, F. Costa Da Silva Almeida, R. Y. Ribeiro, D. C. Schuck, A. K. Jordão, C. R. S. Garcia, *J. Pineal Res.* **2020**, *69*, e12685, https://doi.org/10.1111/jpi.12685.
[25] L. R. C. Mallaupoma, B. K. D. M. Dias, M. K. Singh, R. I. Honorio, M. Nakabashi, C. D. M. Kisukuri, M. W. Paixão, C. R. S. Garcia, *Biomolecules* **2022**, *12*, 638, https://doi.org/10.3390/biom12050638.
[26] J. L. Siqueira-Neto, K. J. Wicht, K. Chibale, J. N. Burrows, D. A. Fidock, E. A. Winzeler, *Nat. Rev. Drug Discovery* **2023**, *22*, 807–826, https://doi.org/10.1038/s41573-023-00772-9.
[27] C. Rasmussen, P. Alonso, P. Ringwald, *Expert Rev. Anti-Infect. Ther.* **2022**, *20*, 353–372, https://doi.org/10.1080/14787210.2021.1962291.
[28] L. Madeira, P. A. Galante, A. Budu, M. F. Azevedo, B. Malnic, C. R. Garcia, *PLoS One* **2008**, *3*, e1889, https://doi.org/10.1371/journal.pone.0001889.
[29] M. S. Moraes, A. Budu, M. K. Singh, L. Borges-Pereira, J. Levano-Garcia, C. Currà, L. Picci, T. Pace, M. Ponzi, T. Pozzan, C. R. S. Garcia, *Sci. Rep.* **2017**, *7*, 9545, https://doi.org/10.1038/s41598-017-09959-8.
[30] B. M. Santos, B. K. M. Dias, M. Nakabashi, C. R. S. Garcia, *Front. Microbiol.* **2021**, *12*, 638869, https://doi.org/10.3389/fmicb.2021.638869.
[31] G. Kokwaro, L. Mwai, A. Nzila, *Expert Opin. Pharmacother.* **2007**, *8*, 75–94, https://doi.org/10.1517/14656566.8.1.75.
[32] S. T. Windle, K. D. Lane, N. B. Gadalla, A. Liu, J. Mu, R. L. Caleon, R. S. Rahman, J. M. Sá, T. E. Wellems, *Int. J. Parasitol. Drugs Drug Resist.* **2020**, *14*, 208–217, https://doi.org/10.1016/j.ijpddr.2020.10.009.
[33] B. M. D. Santos, D. T. G. Gonzaga, F. C. da Silva, V. F. Ferreira, C. R. S. Garcia, *Biomolecules* **2020**, *10*, 1197, https://doi.org/10.3390/biom10081197.

Manuscript received: October 9, 2025